Soybean oil-based green diesel production via catalytic deoxygenation (CDO) technology using low-cost modified dolomite and commercial zeolite-based catalyst

R.S.R.M. Hafriz [a,b,*], S.H. Habib [b], N.A. Raof [c], M.Y. Ong [b], C.C. Seah [b], S.Z. Razali [d], R. Yunus [a], N.M. Razali [b], A. Salmiaton [a,e,*]

[a] Department of Chemical and Environmental Engineering, Faculty of Engineering, Universiti Putra Malaysia, Serdang 43400 UPM, Selangor, Malaysia
[b] Institute of Sustainable Energy, Universiti Tenaga Nasional, Kajang 43000, Selangor, Malaysia
[c] Chemical Engineering Department, Faculty of Engineering, Universiti Teknologi Petronas, Seri Iskandar 32610, Perak, Malaysia
[d] Institute of Nanoscience and Nanotechnology (ION2), Universiti Putra Malaysia, Serdang 43400, Selangor, Malaysia
[e] Sustainable Process Engineering Research Centre, Faculty of Engineering, Universiti Putra Malaysia, Serdang 43400 UPM, Selangor, Malaysia

ARTICLE INFO

ABSTRACT

Green diesel derived from sustainable biomass is an alternative and potential energy source to petroleum fossil fuel replacement in response to reducing carbon footprint and achieving a circular economy, which has sparked public interest and concern in advancing renewable energy development. Catalytic deoxygenation (CDO) is a promising method because it can process a wide variety of feedstocks and produce a diverse range of fuels. The CDO of soybean oil (SO) was executed using a modified low-cost dolomite catalyst denoted as NiO-CD catalyst and its performance has been compared with commercial zeolite heterogeneous-based catalysts such as ZSM-5, HY-zeolite and FCC. The NiO-CD catalyst exhibited exceptional deoxygenation ability, attaining an 88.6 % removal efficiency of oxygenated compounds, markedly surpassing all commercially available zeolite catalysts. The highest degree of CDO of SO via decarboxylation/decarbonylation (deCOx) reaction was achieved due to improvement in particle size, mesoporous structure and the presence of the synergistic effect of modified bi-functional acid-base properties of NiO-CaO/MgO catalyst. To investigate the effect of NiO-CD catalyst loading ranging from 1 to 7 wt%, a One Factor At a Time (OFAT) optimisation study was performed. The current study found that an optimised NiO-CD catalyst loading of 5 wt% yielded the highest green diesel (50.5 wt%) with an 88.63 % hydrocarbon composition. The influence of catalyst loading on deoxygenation activity is significant in green diesel production using NiO-CD catalyst.

Introduction

The use of diesel fuel in various industries and sectors, such as transportation, agriculture, and construction, has led to an increased demand for sustainable fuel options [1,2]. The development of sustainable alternative fuels has received significant interest in recent years due to their environmental benefits and the need to reduce dependency on conventional fossil diesel fuels. When it pertains to alternative fuel options, two commonly discussed choices are green diesel and biodiesel. Green diesel and biodiesel are both considered alternatives to petrol diesel, but they have some key differences. Green diesel is a synthetic renewable hydrocarbon-based diesel that closely resembles petrol diesel

and does not contain aromatic compounds. In contrast, biodiesel is a mixture of alkyl esters of fatty acids derived from vegetable oils or animal fats via a process known as transesterification [3]. Despite the growth prospects of biodiesel, there are several challenges associated with its use in combustion engines [3]. Biodiesel is also confronting technical challenges such as high oxygen content, high corrosivity (high acid value), storage instability, high viscosity, and limited miscibility with conventional fossil diesel fuels, making it an insufficient replacement for petrol diesel [4,5]. Green diesel stands out technically, mainly due to its higher oxidation stability, storage stability, excellent cold flow properties and slightly lower carbon footprint compared to biodiesel [5].

Soybean oil has been extensively utilised as a raw material for manufacturing biofuels despite issues regarding food security and sustainability, which arise from the ready availability and abundance of this feedstock. Soybeans are a highly cultivated crop on a global scale, particularly in countries such as the United States, Brazil, and Argentina. Due to the large production volumes, there is a large quantity of soybean oil that can be used for biofuel production. According to Bergmann *et al.* [6] and Maciel *et al.* [7], Brazil is the second-largest global producer of soybeans, which are currently the primary source used for making biodiesel. Soybean oil accounts for 70 % of the raw material used in the production of Brazilian biodiesel. In addition, Timilsina *et al.* [8] stated that the rise in global pricing of biofuels and feedstocks, such as soybean oil, will lead to an increase in Argentina's gross domestic product and social welfare.

The hydro-processed esters and fatty acids (HEFA) process is capable of converting waste cooking oils and other inexpensive feedstocks into high-quality green diesel and jet fuel blendstocks [9,10]. Hydrogen is a crucial component of the hydrodeoxygenation process, which is a vital step in the production of biofuels, and HEFA relies heavily on it. According to Hebish *et al.* [11], HEFA relies on expensive high-pressure hydrogen, which carries safety hazards. This poses a major challenge to the advancement of hydrogen-free alternatives. However, catalytic deoxygenation can decrease the quantity of hydrogen needed by utilizing decarboxylation and decarbonylation processes [12,13]. This technique could reduce the overall energy requirements and costs associated with the synthesis and use of hydrogen in the manufacturing of biofuels. The catalytic deoxygenation is conducted in an inert environment with a nitrogen purge to avoid oxidation and other undesired side reactions that may occur in the presence of oxygen. Green diesel derived via the deoxygenation of edible and non-edible biomasses has been found to have favourable physical–chemical properties and reduced greenhouse gas emissions compared to biodiesel and petrol diesel [14]. As the industry continues to explore and refine the processes involved in creating green diesel, the potential for more efficient pathways and increased production reliability becomes increasingly apparent.

The catalytic deoxygenation (CDO) is a thermal reaction process which transforms fatty acids/fats into desired hydrocarbons by hydrodeoxygenation, decarboxylation, and decarbonylation process [15]. A variety of factors including the feedstock and conditions of reaction, CDO is typically performed at elevated temperatures and pressure with the inclusion of a metal catalyst. Due to practicality and economic considerations, the catalyst's development influences the degree of selectivity of hydrodeoxygenation, decarboxylation, and decarbonylation process, which is extremely important [16]. A variety of catalysts have been studied for the CDO of plant-based oils, and zeolite (NaY, SBA-15, HZSM-5), metal oxides (MgO and CaO) and activated carbon (AC) are among the primary catalysts used [17]. Commercial Zeolite has been extensively utilized in the production of green diesel because of its remarkable deoxygenation activity. This enables the production of high-quality biofuel without the need for external H_2 sources [18,19]. However, the primary drawback of zeolite-based catalysts is their short catalyst lifetime, which is caused by coke formation during the process [20]. Strong acids, particularly acid catalysts, can cause the formation of coke, which is a carbonaceous residue that can render the catalyst deactivated. Solid base catalysts with fundamental properties can effectively minimize coke formation by following alternative reaction routes and exhibiting reduced propensities to promote polymerization and condensation processes contributing to coke formation. Previous research by Hafriz *et al.* [21] and Romero *et al.* [22] has demonstrated that solid base catalysts, such as CaO and MgO, have the ability to remove oxygen from vegetable oil through decarboxylation (elimination of CO_2) and decarbonylation (elimination of CO) pathways [15]. This is because the catalyst has basic properties that allow it to absorb the CO_2 that is generated during the deoxygenation process, and it also helps to alleviate the issue of coking on the catalyst [23–25]. Besides that, based

on a previous study [26], the acid value of pyrolysis oil is higher for non-catalytic WCO pyrolysis compared to catalytic deoxygenation, with values ranging from 186 mg KOH/g for non-catalytic to 156 mg KOH/g with ZSM-5 catalyst (acid catalyst) and 33 mg KOH/g with CMD900 catalyst (base catalyst). Using base catalysts reduces the acid value by 82 % as compared to using acid catalysts. Oils cracked with acid catalysts have higher carboxylic acid content, which will affect corrosion, cold filter plugging point, and freezing point.

In recent years, the use of dolomite as a potential low-cost catalyst for bio-oil/pyrolysis oil upgrading has gained attention due to its potential as a cheap, natural and environmentally friendly material, high basicity, less toxicity and long catalyst life [26]. Research indicates that dolomite can effectively deoxygenate biofuel, leading to a decrease in the ratio of O/C and ultimately producing high-quality biofuel [27]. For example, the CDO of fatty acid in waste cooking oil (WCO) using a modified dolomite catalyst has been successfully conducted by Buyang *et al.* [28] and Hafriz *et al.* [21] reaction rate and hydrocarbon yield and reduced char formation. A prior investigation by Lin *et al.* [29] discovered that the calcined dolomite catalyst successfully reduced tar yield while removing some oxygen and increasing the H/C ratio slightly. In a different study, Kanchanatip *et al.* [30] successfully modified Thai dolomite with magnesium carbonate ($MgCO_3$) and used it in catalytic pyrolysis of waste cooking oil. The highest pyrolytic product yield of 84.5 % was achieved and the kinetic viscosity test passed compared to the ASTM D445 standard. Substantially, transition metal catalyst over base support has been used in green diesel production from fatty acids due to the selectivity towards decarboxylation and decarbonylation reaction mechanism that results in high oxygen removal [31]. The most common transition metals used in this reaction include Palladium, Platinum and Rhodium catalysts, which possess higher catalytic activity compared to other transition metal base catalysts [32]. However, these high-performance catalysts faced huge economic drawbacks due to its high production cost and recyclability [33]. Hence, many studies have explored the low-cost Nickel catalyst on base support in green diesel and hydrocarbon-like fuel production to mitigate the cost of catalyst [34–36]. These studies also concluded that Nickel catalysts induce a high degree of decarbonylation and decarboxylation (deCOx) reaction mechanism in producing hydrocarbon with lower oxygen composition. The use of Nickel-modified dolomite catalyst in bio-oil production via CDO of pyrolyzed softwood and non-wood was demonstrated in a study by Praserttaweeporn *et al.* [37]. The findings revealed a reduction in acid and sugar levels in the produced biofuel which further favours the production of high-quality liquid hydrocarbon. Nickel-modified dolomite catalyst has also been shown to increase the yield and quality of hydrocarbon-rich bio-oil during co-pyrolysis of plastic waste and biomass [38]. Despite extensive research on dolomite and its transition metal-modified catalysts, there remains a critical gap in exploring the selectivity and efficacy of nickel oxide-dolomite, for deoxygenating soybean oil into high-quality hydrocarbon-rich green fuel. While existing studies highlight the superior performance of dolomite-based catalysts in producing bio-oil through deoxygenation, the novel application of nickel oxide-dolomite in this context is largely unexplored.

This study aims to fill this gap by evaluating the performance of a nickel oxide-modified dolomite catalyst in comparison to conventional commercial zeolite-based catalysts. The selection of zeolite as a reference catalyst in its commercial, unmodified form was based on its extensive industrial application and well-known catalytic properties. Zeolites are renowned for their high acidity, high surface area, and thermal stability, establishing them as a benchmark in several catalytic processes, especially in the petroleum and chemical industries. The choice to refrain from modifying the zeolite with active metals or other improvements is based on the deliberate aim to evaluate the performance of a standard, readily available catalyst in comparison to the new synthesized dolomite catalyst. Preliminary studies conducted by the authors indicated that the nickel oxide-based catalyst shows high conversion and high selectivity for decarboxylation and/or decarboxylation

predominates, suggesting its potential as a groundbreaking catalyst in this field [39]. This work rigorously assesses the catalytic activity of nickel-dolomite in converting soybean oil into green fuel, an area not thoroughly investigated in the literature. This study analyzes how varying catalyst loadings impact the hydrocarbon conversion, the removal efficiency of oxygenated compounds, and overall biofuel quality. This collected data promises to advance the development of sustainable and cost-effective catalysts, setting a new benchmark for producing high-quality hydrocarbon-based biofuels from renewable soybean oil, with potential applications across gasoline, kerosene, and diesel fuels.

Experimental

Chemicals and materials

In this study, soybean oil (SO) was used as an alternative renewable source in green diesel production, and 99.61 % of oxygenated compounds were provided by Scomi Energy Services Bhd. The precise composition of SO was determined using gas chromatography-mass spectrometry (GC–MS) analysis and is presented in Table 1. This SO has the highest content of monounsaturated fatty acid which is 40.14 % oleic acid ($C_{18}H_{34}O_2$, C18:1), followed by 29.35 % saturated fatty acid of palmitic acid, ($C_{16}H_{32}O_2$, C16:0) and 14.14 % saturated fatty acid of stearic acid ($C_{18}H_{36}O_2$, C18:0). In a prior investigation [40], it was determined that 5.7 % of soybean oil contains furan compounds. This presence can be ascribed to either heat processing or extended storage. Likewise, these results aligned with the findings reported by Fan [41] and Javed *et al.* [42]. These chemicals are commonly formed by the process of oxidizing fatty acids and triglycerides. The potential deoxygenation catalyst of Malaysian Dolomite acted as a support catalyst, and it was purchased from Northern Dolomite Sdn. Bhd. Perlis, peninsular Malaysia. While nickel (II) nitrate, $Ni(NO_3)_2 \cdot 6H_2O$ (99.8 %) was utilised as a metal dopant and was bought from Systerm Chemicals Sdn. Bhd. The comparative study employed commercially available zeolite-based catalysts, namely ZSM-5, HY-Zeolite, and FCC, procured from Qingdao Wish Chemicals Co., LTD, located in Shandong, China. Biogas Sdn. Bhd. supplied Industrial Nitrogen gas (N_2) with a purity of 98 %. The chemicals were utilized in their original form without any modification. While dichloromethane with 99 % purity (used for coke washing) and N-hexane with purity > 98 % were purchased from Sigma Aldrich for GC–MS analysis.

Development of NiO-CD catalyst & commercial zeolite-based catalyst

The modified NiO-calcined dolomite (CD) catalyst was synthesized by utilising the precipitation technique to prepare the catalyst. Liquid-liquid blending (precipitation) is widely used to synthesize monometallic and multimetallic oxides. The Malaysian dolomite underwent thermal activation (calcination) at a temperature of 900 °C for 4 h using a Carbolite tube furnace. The calcined Dolomite (CD) was disseminated in 100 ml of deionized water with continuous agitation for 10 min and

Table 1
Soybean oil's composition from GC–MS analysis.

Compositions	Percentage (%)
Oxygenated Compounds:	
Fatty acid	
• Oleic acid (*cis*-9-Octadecanoic acid), $C_{18}H_{34}O_2$, C18:1	40.14
• Palmitic acid (Hexadecanoic acid), $C_{16}H_{32}O_2$, C16:0	29.35
• Stearic acid (Octadecanoic acid), $C_{18}H_{36}O_2$, C18:0	14.14
Furan	5.72
Others (ester, aldehyde, siloxane, etc.)	10.26
Σ	99.61
Hydrocarbon Compound:	
Trisilacyclohexane	0.39

subsequently heated to a temperature of 60 °C. The metal aqueous of 5 wt% $Ni(NO_3)_2 \cdot 6H_2O$ was prepared by dispersing it in deionized water (10 ml) and the resulting solution was then carefully added, one drop at a time, to a suspension of CD. The solution was well-mixed at 60 °C with stirring at 400 rpm for 4 h until a viscous solution was obtained. The obtained viscous sludge-like catalyst was subjected to overnight drying in an oven at a temperature of 120 °C and then it was crushed. The synthesized NiO- calcined dolomite, denoted as NiO-CD, was calcined in a Carbolite horizontal tube furnace at temperatures 900 °C with an average heating rate of 5 °C/min under an air atmosphere for 4 h. The zeolite-based catalysts often used in commercial applications, such as ZSM-5, HY-Zeolite, and FCC, underwent a calcination process at 700 °C in a Carbolite tube furnace for 4 h [43].

Characterization of NiO-CD catalyst & commercial zeolite-based catalyst

The qualitative and quantitative results of synthesized dolomite (XRF & $TPD-CO_2$) and commercial zeolite-based catalysts were determined using XRD, BET, particle size analysis (PSA), and SEM-EDX analysis. Using wavelength dispersive X-ray fluorescence (WDXXRF; Bruker model S8 TIGER), the chemical composition of CD and NiO-CD catalysts was assessed and determined. A CO_2 temperature-programmed desorption (TPD) method was used to determine the basic properties of the synthesised dolomite catalyst. Using a Thermo Finnigan TPD/R/O 1100 equipment from Thermo Fisher Scientific, equipped with a thermal conductivity detector (TCD) and CO_2 as probe molecules, the basicity strength of the synthesised catalyst was measured. The analytical test was conducted by introducing 0.05 g of the synthesised catalyst into a quartz tube reactor with an internal diameter of 6 mm. The synthesised catalysts underwent pre-treatment with nitrogen (N_2) gas flow for 30 min at 250 °C, followed by carbon dioxide (CO_2) gas for 1 h at room temperature to facilitate the adsorption of CO_2 onto the catalytic surfaces. To eliminate the surplus CO_2, the N_2 gas was purged for 30 min at a flow rate of 20 ml/min. The purging of helium gas was carried out at a flow rate of 30 ml min^{-1}, ranging from 60 to 900 °C, with a heating ramp of 10 °C min^{-1}. The basic properties of the synthesized dolomite catalyst were assessed and determined by calculating the integral of the area beneath the provided graph of CO_2 desorption. The catalyst's phase identification and crystalline structure were identified using the Shimadzu XRD-600 instrument. The Cu-Ka radiation was employed for the scan, which was conducted at 40 kV and 40 mA, with a wide area of focus of 2 and 7 kW, respectively. The XRD scanning was performed over a range of 20 to 70°, with a scan rate of 2°/min for 2 h. The Scherrer equation (Eq. (1)) was employed to ascertain the mean crystallite size of the synthesized catalysts.

$$D = \frac{k\lambda}{\beta cos\theta} \tag{1}$$

where k is a constant with a value of 0.98, λ represents the X-ray wavelength which is equal to 1.54178A, β refers to the complete peak width at half maximum in radians of a particularly intensive diffraction peak position and θ represents the Bragg's angle of the 2θ peak. The specific surface area, average pore size, and pore volume distribution of the synthesized catalysts were determined using the Brunauer-Emmett-Teller (BET) method, which involved analysing the Nitrogen isotherm adsorption–desorption data. The analysis was conducted in a vacuum chamber at a temperature of 196 °C, utilising a Thermo-Finnigan Sorpmatic 1990 series apparatus equipped with an N_2 adsorption/ desorption analyzer. Prior to the evaluation, the synthesized catalysts underwent a process of degassing, where they were exposed to a temperature of 150 °C for an extended period of time in order to remove any water and other gases that were adsorbed onto the catalyst surfaces. The determination of particle size was performed using the Particle Size Analyzer (PSA) Nanosizer Nano S, manufactured by Malvern Instruments. The morphology and composition of the elements of the

synthesized catalysts were examined using Scanning Electron Microscopy (SEM) coupled with electron dispersive X-ray spectroscopy (EDX). To get clear SEM images, the synthesized catalysts were examined using an SEM JOEL 6400 electron microscope, which operated at an acceleration voltage of 40 kV.

Catalytic deoxygenation (CDO) of soybean Oil (SO)

As illustrated in Fig. 1, the CDO of the SO reaction was carried out in a mechanically stirred 1L fractionation catalytic system equipped with a temperature controller. Initially, 150 g of SO and approximately 7.5 g of catalyst, which is equivalent to 5 wt%, were introduced into a three-neck flask reactor with a volume of 1000 ml. The reaction mixture in the flask reactor was continuously stirred at a speed of 400 rpm. In order to maintain an environment free of oxygen, the reactor was purged with inert industrial N_2 gas at a flow rate of 50 cm^3/min before the heating process. The temperature requires 18–20 min to attain the target temperature of 400 °C with a tolerance of ± 10 °C. The CDO reaction of SO was conducted for 30 min. The one-factor-at-a-time (OFAT) technique was employed to investigate the impact of catalyst loading (1, 3, 5 and 7 wt%) on the CDO system. The vapour/volatile product generated was condensed in the collected flask by using external circulating cooling water. The gas release was determined by calculating the difference between the weight of coke remaining in the flask reactor and the weight of the liquid product generated by the collecting flask based on the variations between the feedstock, coke and liquid product. The gas product was discharged through the gas outlet without undergoing any analysis. According to a prior study [26], the GC-TCD method analysis can identify the general composition of gaseous compounds such as H_2, O_2, CO, CH_4, and CO_2. The production of CO_2 (20.56 %) and CO (3.56 %) occurred upon the decarboxylation and decarboxylation of WCO during the pyrolysis using calcined Malaysia dolomite, CMD900. The low concentration of oxygenated compounds using the CMD900 catalyst allows for clear observation of these reactions in the composition profile of pyrolysis oil. The formation of three phases in the liquid product could be observed using a NiO-CD catalyst. The upper phase was pyrolysis oil denoted as green diesel (GD), the second phase involved the formation of soap, while the last phase consisted of an acid phase. The soap formation was isolated using filtration using filter paper, while the acid phase was separated. The chemical composition of green diesel was determined using GC–MS analysis. The SO-based green diesel and the conversion of SO were calculated through mass balance using Eqs. (2) and (3), respectively [44].

$$Yield\ of\ green\ diesel(wt\%) = \frac{mass\ of\ green\ diesel(g)}{mass\ of\ SO\ used(g)} x100\% \qquad (2)$$

$$Conversion\ of\ SO(wt\%)$$
$$= \frac{mass\ of\ SO(g) - \Sigma(mass\ of\ coke + unreacted\ oil)(g)}{mass\ of\ SO(g)} x100\% \qquad (3)$$

Product analysis

The diluted green diesel (GD) with n-hexane was evaluated quantitatively using gas chromatography. The gas chromatography instrument used was a Shimadzu GC-14B, which was equipped with a ZB-5MS column. The dimensions of the column were as follows: length of 30 m, inner diameter of 0.25 mm, and film thickness of 0.25 μm. The analysis was performed in a split mode. A volume of 2 μm of liquid sample was introduced into the GC column with the utilising helium gas as the carrier gas. The oven was initially adjusted to maintain a temperature of 40 °C for 3 min. Subsequently, the temperature was increased at a rate of 7 °C/min until it reached 300 °C. The temperature was then maintained at 300 °C for 5 min. The injection temperature was configured to 250 °C while maintaining a flow rate of 3.0 ml/min. The diffraction peaks observed in the GC–MS spectra of compounds, particularly hydrocarbons (C_8-C_{24}) and oxygenated compounds, were identified using the National Institute of Standards and Testing (NIST) library. Although GC–MS analysis does not produce exact quantitative results for compounds, it is possible to compare the selectivity and yield of hydrocarbon products by examining the peak areas on the chromatograph. The peak area of a compound is directly proportional to its quantity and the relative content of the product [45,46]. To ensure the replicability of the findings, the tests were repeated three times, and the average values of the peak area and peak area percentage were computed. The key products were identified and differentiated using a probability match of 95 % or above [21].

The hydrocarbon yield (H_C) of green diesel was calculated using Eq. (4).

$$H_C = \frac{\sum Area\ of\ hydrocarbon\ compound(C8 - C24)}{\sum area\ of\ the\ product} \times 100\% \qquad (4)$$

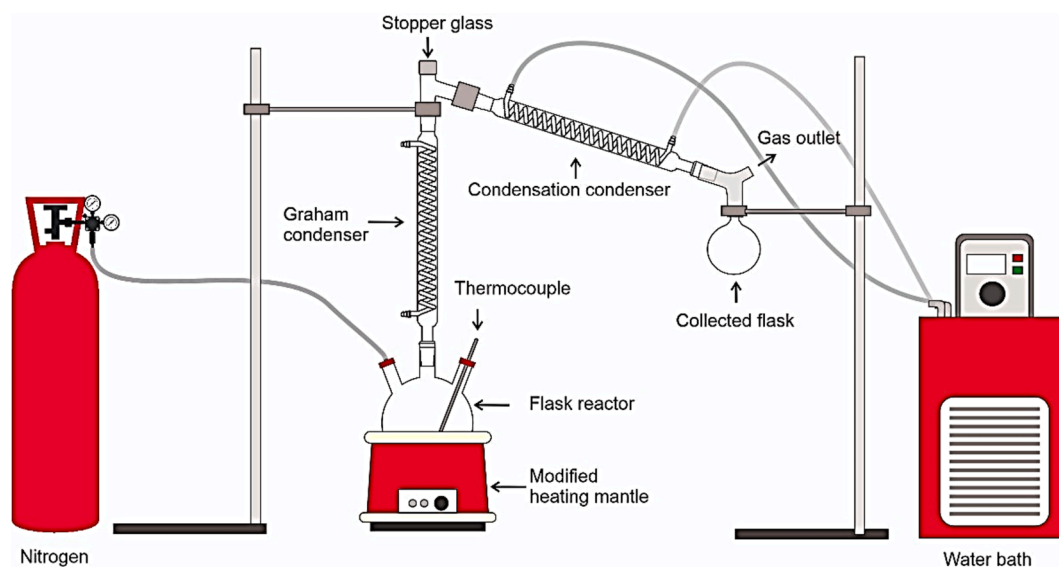The hydrocarbon selectivity (H_s) of green diesel was determined using Eq. (5).

Fig. 1. Schematic diagram of fractionated cracking for CDO reaction [44].

$$H_s = \frac{\sum Area\ of\ the\ desired\ hydrocarbon\ fraction}{\sum area\ of\ hydrocarbon\ compounds} \times 100\% \quad (5)$$

The percentage elimination of the oxygenated compound (O_c) was determined using Eq. (6) [21].

$$O_C = \frac{\Sigma Area\ of\ oxygenated\ compound\ SO - \Sigma Area\ of\ oxygenated\ compound\ GD}{\Sigma Area\ of\ oxygenated\ compound\ of\ SO}$$
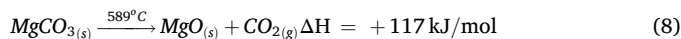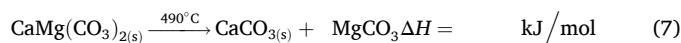$$x100\%$$
$$(6)$$

Results and discussions

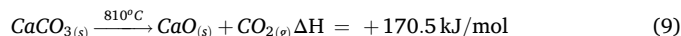*The catalyst morphology and physicochemical properties*

The XRD of catalyst samples are presented in Fig. 2. XRD diffractograms were utilised to determine the crystallographic phase of both synthesized Malaysian dolomite and commercial zeolite-based catalysts. After thermal activation at 900 °C for 4 h, the increased diffraction peak indicates the absence of diffraction lines associated with carbonate species, since they were released in the form of CO_2 for CD catalyst. CaO and MgO are the main compositions observed on the XRD pattern of CD catalysts. The intensified peaks present in CD catalyst which matched to CaO at 2θ = 32.34°, 34.18°, 37.52°, 54.02°, 64.28° and 67.52° with JCPDS File: 37-1497 and MgO diffraction peaks at 2θ = 43.08° and 62.46° (JCPDS File: 71-1176), which agreed with finding by Correia *et al.* [47], Muhammad *et al.* [48] & Hafriz *et al.* [21]. As reported by Hafriz *et al.* [26], Resio [49] & Taufiq Yap *et al.* [50], the disintegration

of CaMg(CO$_3$)$_2$, also known as dolomite, was observed through the existence of distinct peaks corresponding to the CaO and MgO phases. These peaks appeared at different stages of thermal temperature, as determined by Derivative Thermogravimetry (DTG) analysis. Reaction mechanisms in Eq. (7), (8) and (9) delineate the sequential breakdown that takes place at various thermal temperatures, based on the enthalpy energy of each constituent present in the thermal activation of the dolomite catalyst.

First Peak:

$$CaMg(CO_3)_{2(s)} \xrightarrow{490°C} CaCO_{3(s)} + MgCO_3 \Delta H = \qquad kJ\Big/mol \quad (7)$$

$$MgCO_{3(s)} \xrightarrow{589^oC} MgO_{(s)} + CO_{2(g)} \Delta H = +117\,kJ/mol \quad (8)$$

Second Peak:

$$CaCO_{3(s)} \xrightarrow{810^oC} CaO_{(s)} + CO_{2(g)} \Delta H = +170.5\,kJ/mol \quad (9)$$

The appearance of the CaO and MgO phase after thermal activation at 900 °C, proves that the calcined dolomite (CD) catalyst was a very stable compound of catalyst. Meanwhile, precipitation of NiO onto calcined dolomite as a support catalyst (NiO-CD) was successfully dispersed by the emergence of a distinct new NiO crystal peak at an angle of 2θ = 47°. It was confirmed that the Nickel distribution onto the dolomite catalyst (NiO-CD) will reduce the intensity peak of the CaO and MgO phases as compared to the CD catalyst. Under thermal activation at 700 °C for 4 h, the X-ray diffraction (XRD) pattern of commercial zeolite-based catalyst exhibited the typical characteristic peak of zeolite-based catalyst, as
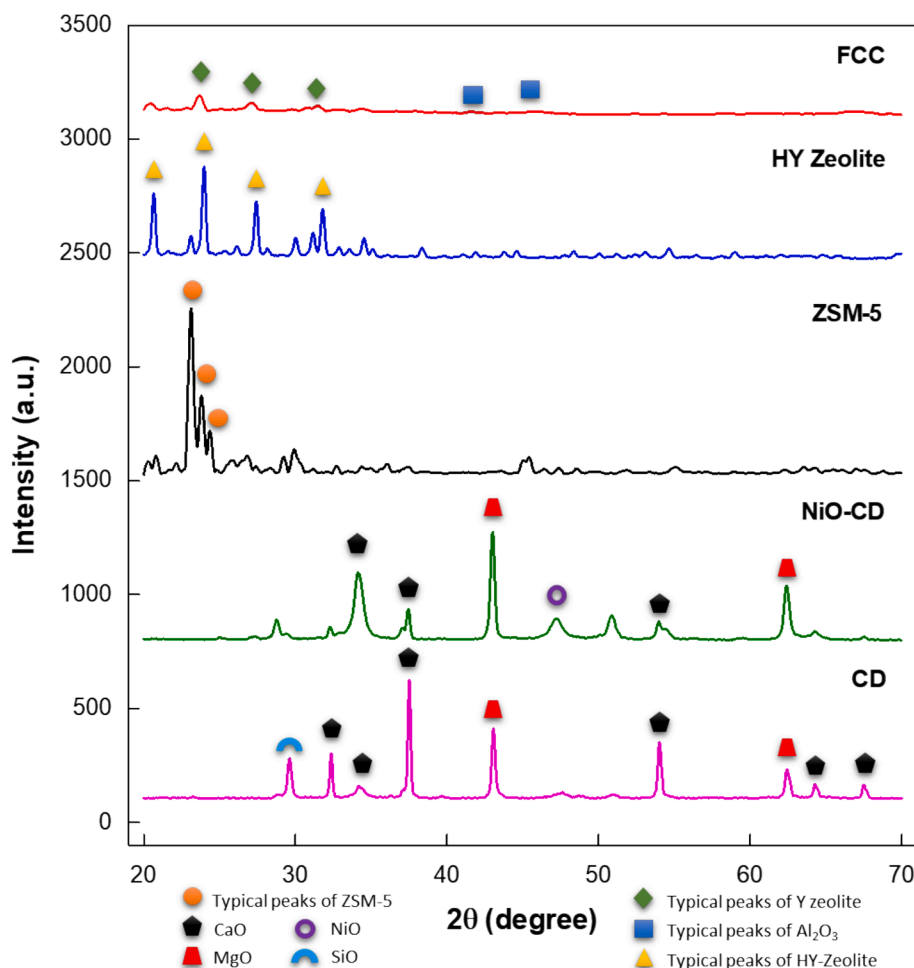

Fig. 2. XRD pattern of dolomite and commercial zeolite-based catalyst.

illustrated in Fig. 2. The peak in the diffraction spectrum corresponding to the commercial ZSM-5 catalyst structure was observed clearly at $2\theta = 23.1°$, $23.82°$ and $24.32°$. The typical diffraction peak pattern observed is in agreement with the data found by Li *et al.* [51] and Emori *et al.* [52]. While the typical peak of HY-zeolite catalyst was observed at $2\theta = 20.66°$, $23.98°$, $27.42°$ and $31.78°$ which is completely matched with the diffraction peak of HY-zeolite verified by Ramli *et al.* [53] and Ameen *et al.* [54]. For XRD pattern of FCC displayed the typical characteristic of Y-type zeolite at $23.7°$, $27.1°$ and $31.54°$ and characteristic peaks of Al_2O_3 at $2\theta = 42.43°$ and $45.68°$. This typical characteristic peak observed had a close resemblance to the conventional zeolite Y phase (JPDS card No. 75–1551) and Al_2O_3 peaks as reported by Xu & Zhang, [55] and Chen *et al.* [56]. In addition, as reported by Chen *et al.* [56], thermal activation or calcination treatment did not influence the FCC catalyst due to no significant changes in XRD patterns between calcined FCC and uncalcined FCC. The XRD pattern observed in all commercial zeolite-based catalysts showed that the synthesized catalysts did not contain any detectable quantity of non-zeolitic crystal phases after thermal activation at 700 °C due to the absence of additional peaks pattern in Fig. 2.

The crystallite size of metal oxide presence in developed catalysts was indentified by using Debyee-Scherrer's equation (Eq. (1)) and was tabulated in Table 2. The successful Nickel dispersion onto dolomite support can be observed through the formation of NiO crystallite size on the NiO-CD catalyst due to the presence of a new intensified peak at $2\theta = 47.22°$. Besides that, the CaO and MgO crystallite size reduction of the NiO-CD catalyst at $2\theta = 37.5°$ and $43°$ as compared to CD catalyst demonstrates the existence of the NiO phase. This finding was in line with the report by Yu *et al.* [57], with the introduction of the transition metal of Nickel, the strength of the XRD peak for the synthesised MCM-41 catalyst showed a minor drop, suggesting that the addition of Nickel did not impact the ordered structure of the MCM-41 support. However, the crystallinity of MCM-41 was slightly diminished. While Prihadiyono *et al.* [58] found out that, the crystallinity of the components in the Natural Zeolite catalyst decreased when nickel metals were loaded utilising the impregnation method of catalyst preparation. In zeolite-based catalysts, the crystallite size of SiO_2/Al_2O_3 can be calculated with intensified peaks at $2\theta = 23.1°$, $23.7°$ and $23.9°$ for ZSM-5, FCC and HY-zeolite catalysts, respectively.

The physicochemical properties of the synthesised dolomite catalyst and the commercial zeolite catalyst were assessed using BET and PSA analysis, as shown in Table 3. The surface area of the NiO-CD catalyst (18.20 m^2/g) rose progressively after incorporating and dispersing nickel, in comparison to the CD catalyst (6.46 m^2/g). Nickel particles are finely dispersed on a dolomite catalyst support, which leads to an increased effective surface area for the synthesized NiO-CD catalyst. The

Table 2
Physicochemical properties of synthesized dolomite catalyst and commercial zeolite-based catalyst.

Characterization	Crystallite size of CaO[a]	Crystallite size of MgO[b]	Crystallite size of NiO[c]	Crystallite size of SiO_2/Al_2O_3[d]
CD	39.77	33.04	–	–
NiO-CD	27.82	28.62	27.52	–
ZSM-5	–	–	–	20.26
HY-Zeolite	–	–	–	29.26
FCC	–	–	–	12.57

[a] Calculated using Scherrer equation based on XRD diffraction pattern of CaO (37.5°).
[b] Calculated using Scherrer equation based on XRD diffraction pattern of MgO (43°).
[c] Calculated using Scherrer equation based on XRD diffraction pattern of NiO (47.22°).
[d] Calculated using Scherrer equation based on XRD diffraction pattern of SiO_2/Al_2O_3.

Table 3
Physicochemical properties of synthesized dolomite catalyst and commercial zeolite-based catalyst.

Catalyst	BET surface area m^2/g	Pore volume cm^3/g	Average pore diameter nm	Mean particle size (μm)
CD	6.46	0.28	85.20	42.88
NiO-CD	18.20	0.22	48.20	21.23
ZSM-5	335.40	0.21	1.27	7.54
HY-Zeolite	515.10	0.33	1.29	8.54
FCC	215.70	0.40	3.69	69.82

surface area increased due to the successful dispersion of Nickel using precipitation techniques of catalyst preparation. A greater surface area facilitates an increased number of active sites for the adsorption of reactant molecules of SO and their involvement in deoxygenation processes. This leads to increased catalytic activity of synthesized catalysts and faster deoxygenation reaction rates. Meanwhile, for commercial zeolite-based catalysts, the surface area was extremely higher due to zeolite's unique structure such as highly ordered and regular crystal lattice structure. This regularity allows for a consistent and repeatable arrangement of active sites on the surface, maximizing the available of effective surface area for catalysis. As reported by Al-Jammal *et al.* [59], zeolite-based catalysts have been employed in industrial facilities to facilitate cracking and deoxygenation reactions. This is attributed to their expansive surface area, precisely defined pore architectures with molecular-sized channels and cavities, and shape selectivity. As reported by Yuan *et al.* [60], the pore volume of a catalyst is essential because it can affect the catalyst's ability to adsorb reactants, provide active sites for catalysis, and facilitate mass transport within the catalyst material. As tabulated in Table 3, the pore volume for the NiO-CD catalyst was reduced due to the dispersion of nickel onto dolomite catalyst support as compared to CD catalyst. In comparison to catalysts based on commercial zeolites, the pore volume of the NiO-CD catalyst was smaller than HY-zeolite and FCC catalysts. Catalysts with a higher pore volume often have more accessible active sites and better mass transport properties, which can enhance their performance in deoxygenation reactions. The mean pore diameter of a synthesized catalyst as mentioned in Table 3 will provide information about the accessibility of pores, and the transport of fluids or gases through a synthesized catalyst, and it will also classify the synthesized catalyst into different types of porous catalysts. As tabulated in Table 3, ZSM-5 and HY-zeolite were categorised as microporous catalyst materials since their pore size is smaller than 2 nm, FCC and NiO-CD were categorised as mesoporous catalytic materials with a pore size ranging from 2 to 50 nm, and CD catalyst with pore size greater than 50 nm was classified in macroporous catalytic materials. The successful Nickel dispersion onto the dolomite catalyst improves the network connectivity, resulting in an observable increase in surface area and formation of mesoporosity size range as observed in Table 3 for NiO-CD catalyst. The mesoporous catalyst typically has a high surface area due to its well-structured and interconnected pores. The significant surface area facilitates a greater number of active sites for catalytic reactions, hence enhancing the efficacy of the catalyst as compared to CD catalysts. As reported by Ooi *et al.* [61], mesoporosity significantly influences liquid-phase catalysis because of its substantial surface area and expansive pore structure, which mitigates diffusion issues. Besides that, mesoporous catalysts can mitigate mass transfer limitations that are common in reactions involving bulky reactants. The relatively large and interconnected pores allow reactants and products to diffuse more readily through the catalyst, reducing diffusion limitations. This is aligned with the study revealed by Wang *et al.* [62], the mesoporous structure of zeolite-based catalyst could affect and facilitate molecule diffusion of substrate molecule and improve reaction efficiency by enhancing mass transfer.

Table 3 revealed that the dispersion of nickel onto calcined dolomite,

CD catalyst was successful improved the mean particle size of NiO-CD catalyst from 42.88 μm to 21.23 μm. However, in comparison with a commercially available catalyst based on zeolite, ZSM-5 and HY-Zeolite, both particle size was more smaller with 7.54 μm and 8.54 μm, respectively. The small size of catalyst particle with a high surface area-to-volume ratio will provide more active sites for reactants to adsorb and react, which can enhance catalytic activity. This improved interaction between the reactants and catalyst by promoting a more efficient and sufficient conversion process, resulting in a higher yield of the desired products. This is known as the 'size effect' of nanoparticle catalysts. As reported by Qureshi et al. [63], smaller particle sizes of synthesized tend to yield higher-quality products and greater product yields as compared to those catalysts with larger particle sizes. Besides that, in economic considerations, smaller catalyst particles with a high surface area may allow for the use of less catalyst material while maintaining the desired catalytic activity. This can have an economic impact, particularly if the catalyst is expensive.

The surface morphologies of the synthesized catalyst of dolomite and commercial zeolite-based catalyst under 10 K and 30 K times of magnification are depicted in Fig. 3. The CD catalyst exhibited a finer particle size and a more uniform size distribution, forming loose aggregates of round-shaped particles, as depicted in Fig. 3(a & b). As compared to the morphology of the CD catalyst, the successful dispersion of nickel can be observed due to alteration of the porosity and surface area of dolomite support as shown in Fig. 3(c & d). Nickel particles can increase surface area and its roughness, creating more active sites for adsorption and reactions which directly enhance the catalytic activity of synthesized dolomite catalyst. The observed phenomenon could be attributed to the interaction between NiO (metal dopant) and dolomite, acting as a catalytic support. This result was aligned with the physisorption analysis of the NiO-CD catalyst where there was an increase in the BET surface area, whereas the pore size dropped as tabulated in Table 3. In addition, the dispersion of the catalyst doped with active nickel has modified the morphological structure of the CD catalyst. This alteration is evident by the enhanced crystallinity of the doped NiO, as shown in Table 2. Besides that, based on previous studies, NiO-CMD catalyst caused a notable transformation in the surface morphology. The original cuboid-shaped CaO structure, which had scattered small circular shapes of MgO, changed into a large spherical structure with different orientations after the interaction of the multiphase NiO-CaO/MgO and the dispersion of nickel onto the CMD catalyst surface [44].

Fig. 3(e & f) illustrates the surface morphology structure of the ZSM-5 zeolite with disordered hexagonal plate-like morphology. The hexagonal plate-like morphology structure of the ZSM-5 catalyst can offer advantages in catalytic applications because it can provide a large effective surface area with accessible active sites which aligns with the finding on BET surface area of ZSM-5 (335.40 m^2/g) in Table 3. This can enhance catalytic performance, especially in reactions where shape-selective properties are crucial, such as in the conversion of large molecules like bulky hydrocarbons. According to study conducted by Basir et al. [64], the utilisation of Zeolite ZSM-5 as a catalyst in the conversion of jet biofuel range hydrocarbons from palm oil is effective in enhancing petrol octane number and light olefins. This is attributed to the distinctive morphology, shape selective properties, strong acidity, and hydrothermal stability of Zeolite ZSM-5. Meanwhile, Fig. 3(g & h) displays the SEM images of the HY-zeolite with the presence of well-defined octagonal-like morphology. This kind of the morphology of HY-zeolite, characterised by a consistent shape and distinct size has also been documented by Dadashi et al. [65] and Ren et al. [66]. Based on Fig. 3(i & j), the presence of fines and tiny spherical particles can be observed in the morphology of the FCC catalyst which directly shows a high specific surface area obtained by the FCC catalyst as mentioned in Table 3. As described by Ji et al. [67], the morphology of the synthesised zeolite catalyst directly affects the effectiveness of diffusion, the length of diffusion, and the accessibility of acid sites which indirectly facilitate the

catalytic reaction efficiency of catalyst in hydrocarbon cracking.

Table 4 exhibits the elemental and metal oxide composition of synthesized dolomite catalyst and commercial zeolite-based catalyst using Energy Dispersive X-ray (EDX) and X-ray Fluorescence (XRF) analysis, respectively. During EDX analysis, the catalyst's individual elements emit X-rays at specific energy levels (wavelengths), which are unique to that element. The magnitude of these X-rays is directly proportional to the concentration of the respective element in the catalyst sample, as outlined in Table 4. Table 4 indicates that the primary components of CD and NiO-CD catalysts were calcium (Ca), magnesium (Mg), and oxygen (O). X-ray fluorescence (XRF) analysis in Table 4 clearly shows that the metal oxide composition of synthesized dolomite catalyst consists of over 69–75 % CaO and around 20–30 % MgO. This is because CaO and MgO were formed as a result of calcination at 900 °C. This is consistent with the findings of the XRD analysis (Fig. 2) as a result of the prominent peaks observed for CaO and MgO. The features of Mg and Ca metals have been extensively studied in order to enhance the quality of green diesel produced by the deoxygenation reaction, owing to their distinctive alkaline characteristics. Previous research has shown that the presence of MgO and CaO in the catalytic deoxygenation of waste cooking oil results in a more effective method of removing oxygen in the form of CO_2 [39]. In addition, as revealed by Lin et al. [29], CaO facilitates oxygen removal by efficiently absorbing CO_2 in the gaseous phase. Additionally, CaO can directly capture CO_2-like compounds in the liquid produced, providing an effective deoxygenation pathway in the biomass-to-liquid (BTL) conversion process. Besides that, Tani et al. [68] discovered that the catalysts supported by MgO enhanced the quality of the green diesel by reducing the acid value and iodine value. Furthermore, the resulting product was effectively utilised in diesel engines. As observed in Table 4, the discovery of Nickel content throughout the NiO-CD catalyst proves that the 5 wt% of Nickel was successfully dispersed onto the CD catalyst surface using precipitation techniques. 93.4 % of the successful rate of metal dispersion can be calculated based on nickel content and 82.8 % of NiO formation, as shown in Table 4. The observations of NiO production in the XRF analysis provide convincing evidence of the effective dispersion of nickel onto the dolomite catalyst. The observation of well-defined NiO peaks confirms that nickel has been successfully incorporated into the catalyst matrix. Moreover, the EDX study confirms this discovery by demonstrating consistent nickel dispersion over the dolomite surface, therefore illustrating the effective incorporation of nickel as NiO. Transition metal oxide (TMO), such as NiO, is an effective catalyst promoter. It serves as a viable substitute for noble metals like palladium (Pd) and platinum (Pt) in catalytic cracking applications. As reported by Chen et al. [69], TMO significantly influenced the adjustment of product selectivity towards monofunctional hydrocarbon intermediates by a deoxygenation reaction, which subsequently advanced towards the desired hydrocarbon-like chain. As reported by previous studies, the inclusion of NiO species enhances the presence of an acidic site in the catalyst system, whereas the combined effects of bi-functional NiO-CaO/MgO (acid-base) features can be achieved using precipitation procedures during catalyst preparation [44]. Besides that, the EDX examination results indicate that the commercial zeolite-based catalyst mostly consists of the components Si, Al, O, and C. The disparities discovered in the Si/Al ratio will determine the categorization of zeolite catalysts. The activity of the zeolite-based catalyst can be influenced by the Si/Al ratio. As reported by Daligaux et al. [70], the reactivity of zeolite is attributed to the existence of surface acid sites, which are influenced by their composition, specifically the Si/Al ratio, determining both their quantity and strength. The Si/Al ratio of commercial zeolite-based catalysts followed the order ZSM-5 > HY-Zeolite > FCC, as indicated in Table 4. Typically, a greater Si/Al ratio is correlated with increased catalyst activity, resulting in enhanced efficiency and accelerated hydroprocessing reaction [71,72]. This is because a high Si/Al ratio has been discovered to enhance the catalyst's stability and durability, making it more resistant to framework degradation [73]. In addition, silicon (Si) content helps to create a more acidic
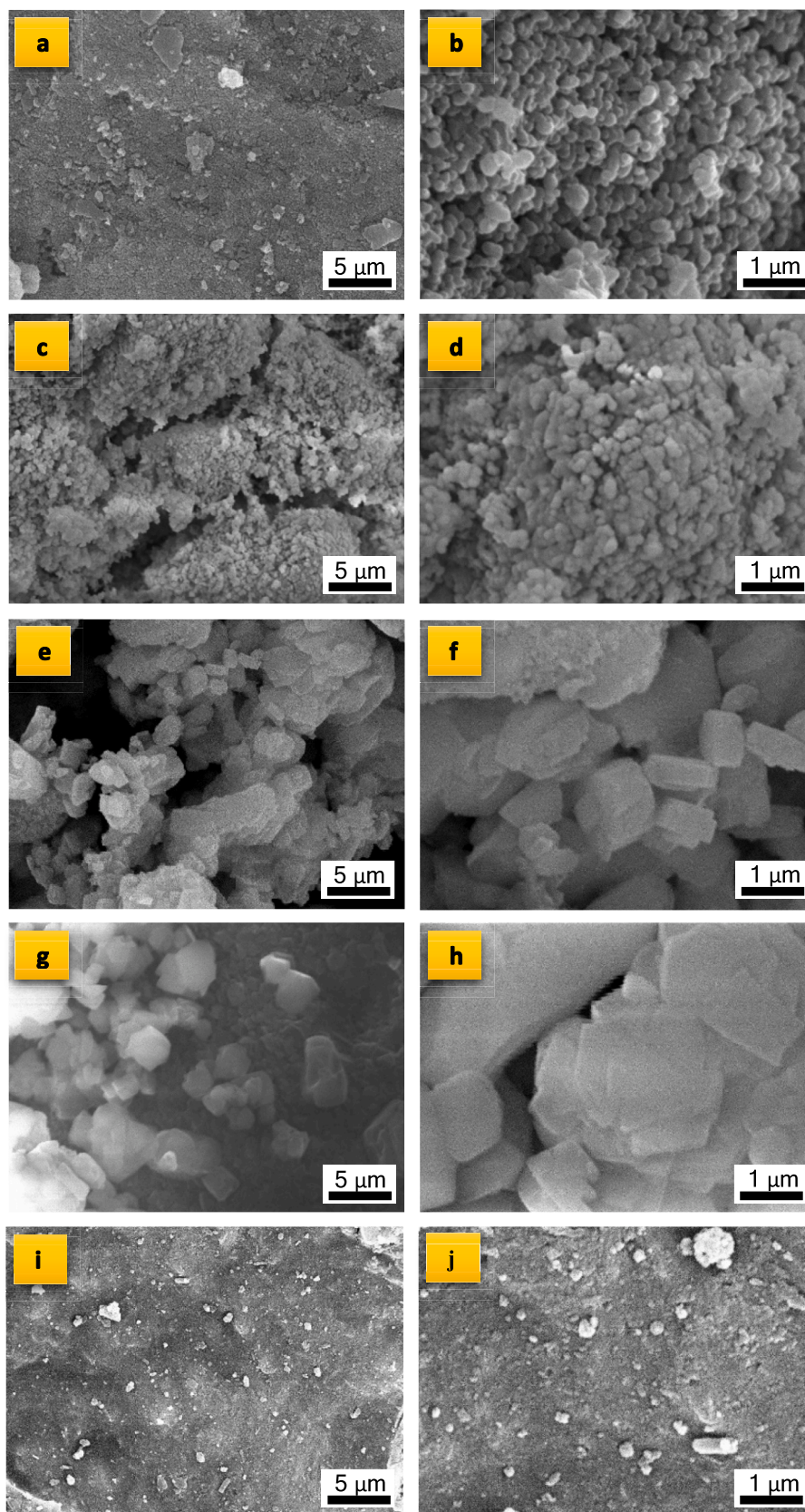
Fig. 3. SEM images of CD (a, b), NiO-CD (c,d), ZSM-5 (e, f), HY-Zeolite (g, h) and FCC (i, j).

Table 4
Elemental and metal oxide composition of synthesized dolomite catalyst and commercial zeolites-based catalysts.

Catalysts	Elemental composition (wt.%)								
	Carbon (C)	Oxygen (O)	Magnesium (Mg)	Calcium (Ca)	Nickel (Ni)	Sodium (Na)	Silicon (Si)	Aluminium (Al)	Si/Al ratio
CD	7.53	42.95	18.35	31.17	n.d	n.d	n.d	n.d	n.d
NiO-CD	8.86	35.12	24.97	26.38	4.67	n.d	n.d	n.d	n.d
ZSM-5	15.54	54.78	n.d	0.03	n.d	n.d	27.08	2.56	18.00
HY-Zeolite	6.80	50.04	n.d	0.08	n.d	0.36	32.03	10.69	3.00
FCC	20.96	48.34	0.09	0.08	n.d	n.d	12.26	18.27	0.67
	Metal Oxide Composition (%)								
Catalyst	CaO			MgO		Fe_2O_3		NiO	
CD	69.30			30.20		0.50		n.d	
NiO-CD	74.60			20.90		0.36		4.14	

n.d: not detected.

site catalyst, which can contribute to better cracking by boosting the production of green diesel and promoting the selectivity of desired reactions [74,75]. Besides that, catalysts with higher Si/Al ratios often require less in situ hydrogen for the hydroprocessing reactions in the catalytic cracking process. This can be advantageous in helping in situ hydrogen consumption in the deoxygenation process under the flow of nitrogen gas, making it a more effective and eco-friendly catalyst. In addition, the Si/Al ratio has the potential to influence the stability as well as the lifespan of the zeolite-based catalyst. Catalysts possessing a greater Si/Al ratio exhibit enhanced resilience against deactivation caused by impurities or the creation of coke during reactions, resulting in extended lifespans of the catalysts. As discovered by Li *et al.* [76] and Li *et al.* [77], the high-silica ZSM-5 catalyst with a Si/Al ratio of 181 showed excellent performance in the methanol-to-propane (MTP) reaction. The low acid density, resulting from the high Si/Al ratio, extends the lifespan of zeolites in the methanol to hydrocarbon (MTH) process.

The successful dispersion of Nickel Oxide (NiO) onto the dolomite catalyst, as determined by X-ray Diffraction (XRD) and Energy-Dispersive X-ray Spectroscopy (EDX) analyses, offers significant understanding of the structural and compositional changes that contribute to the development of bi-functional acid-base characteristics in the catalyst. The NiO crystalline phases in the modified dolomite catalyst indicate that NiO has been dispersed successfully, unlike the Ni element identified via EDX analysis. Dolomite, a naturally occurring mineral consisting of calcium magnesium carbonate, possesses inherent alkaline

sites due to the presence of carbonate groups. The dolomite structure inherently possesses a basic site. The basicity of dolomite is attributed to the presence of MgO and CaO, as these oxides have a propensity to give electron pairs. When NiO is spread out across the surface of dolomite, more acidic sites are created. NiO, a transition metal oxide, exhibits Lewis acid behavior by its capacity to take electron pairs. The interaction between the fundamental sites on dolomite and the acidic sites introduced by NiO results in the formation of the bi-functional properties of the catalyst. The presence of desorption peaks at high-temperature regions, 722 °C (1.73×10^{21} atom/g) for CD and 822 °C (4.40×10^{21} atom/g) for the NiO-CD catalyst, indicate that both catalysts in Fig. 4 displayed significant basicity. Furthermore, the graph pattern of the NiO-CD catalyst exhibits a faint peak around 546 °C, indicating a CO_2 desorbed activity of around 2.75×10^{20} atom/g. As shown in Fig. 4, the dispersion of NiO onto the dolomite catalyst has increased the modified catalyst's basic strength, which contradicts the study reported by Shamsuddin *et al.* [78]. An investigation revealed that the acidity of NiO reduced the number of basic sites (nCO_2) in the catalyst. These phenomena arise due to the limited access of CO_2 to basic sites on dolomite, which is impeded by NiO particles. This obstruction co-occurs with a reduction in the specific surface area of the dolomite material. Based on previous studies [40], the dispersion of NiO can alter the dolomite catalyst's surface structure. Altered surface morphology can influence the spatial arrangement and strength of acidic sites. Furthermore, NiO can act as either an electron donor or acceptor,
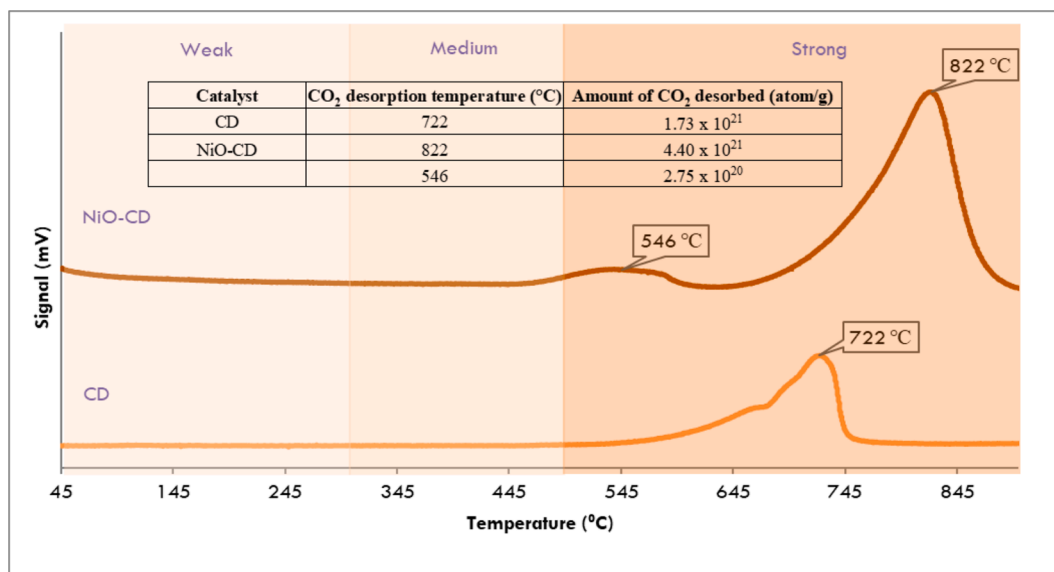
Fig. 4. TPD-CO_2 profiles of synthesized dolomite catalyst.

therefore impacting the electron density inherent in the dolomite catalyst. Alterations in electron density can affect dolomite's acid-base properties, reducing the number and intensity of acidic sites in the NiO–CD catalyst.

Effect of using different catalysts

Product distribution using mass balance

Fig. 5 shows the product distribution and conversions of SO under thermal (without catalyst) and under CDO (different types of catalyst used) which are measured based on weight percentage (wt.%) via mass balance. The deoxygenation of SO was conducted using a 5 wt% catalyst loading, a reaction temperature of 400 °C, and a reaction time of 30 min. The reaction was carried out under an inert N_2 flow with a stirring rate of 400 rpm. The conversion of SO into liquid and gas products was higher using ZSM-5 catalyst (86.7 wt%) followed by NiO-CD (79 wt%), HY-Zeolite (78.3 wt%), thermal (75.6 wt%) and FCC (67 wt%). Commercial acid catalysts, specifically ZSM-5 (56.5 wt%) and HY-Zeolite (55.9 wt%) generated a high yield of pyrolysis oil or green diesel (GD) followed by NiO-CD (50.5 wt%), FCC (44.1 wt%) and thermal (37.6 wt%). This finding shows that ZSM-5 and HY-Zeolite are the best catalysts for cracking high molecular weight SO triglycerides into light molecular weight hydrocarbons in liquid and gas form due to the high significant conversion of SO and green diesel yield via CDO, as tabulated in Fig. 5. This is in line with the study carried out by Scaldaferri and Pasa [79], where zeolite ZSM-5 led to a high yield of green diesel via CDO of SO under a hydrogen-free process. This outcome can be attributed to the abundant acid sites present in the zeolite, which facilitated a rapid occurrence of cracking events. The exceptional conversion of SO and the remarkable yield of green diesel were attributed to the superior surface area and fine particle size of ZSM-5 and HY-Zeolite in comparison to alternative catalysts. These features will enhance the availability of active sites for catalytic reactions. That means there are more reactants of SO that can interact with the catalytic sites, leading to enhanced catalytic activity and increased deoxygenation reaction rates. Besides that, fine particles have shorter diffusion paths for the reactant of SO and products within this zeolite structure. This leads to reduced diffusion constraints and more efficient utilization of the catalytic sites in the CDO

of SO. Besides that, the zeolite-based catalyst's abundance of acid sites on its surface facilitates the hydrolysis and cracking reactions, resulting in a substantial production of green diesel. As discovered by Valle et al. [80], the strong acid sites of zeolite catalysts, namely HZSM-5, are responsible for the high activity in converting oxygenates from bio-oil (derived from pine sawdust) into hydrocarbons through deoxygenation.

Meanwhile, as observed in Fig. 5, the NiO-CD catalyst exhibited excellent performance as a commercially viable catalyst based on zeolite, resulting in high yields of green diesel. This can be attributed to the synergistic effect of its bi-functional acid-base characteristics of NiO-CaO/MgO catalyst. As discovered by Shamsuddin et al. [78] and Hafriz et al. [39], the dispersion of NiO species on the surface of the dolomite support catalyst will provide strong acidic sites and indirectly form synergistic impact due to its bi-functional acid-base properties. The success of Nickel dispersion onto the dolomite surface provides an active site where it can promote efficient redox reactions via CDO by facilitating the transfer of electrons between species, which is fundamental to redox processes. The dispersion of nickel can facilitate the addition or removal of in situ hydrogen (H_2) atoms from SO which slightly improves the catalytic activity in hydrogenation and dehydrogenation reactions for converting to hydrocarbon product. According to Gosselink et al. [81] and Hermida et al. [82], The basicity qualities had a vital role in preventing the development of coke and facilitating the breaking of C-O bonds through decarboxylation reactions. On the other hand, acidity was necessary to commence the breaking of C-C bonds through DO reactions. As compared to non-catalytic reactions via thermal cracking, the presence of a catalyst enhances the conversion of SO and the production of green diesel by providing a surface or active site where the SO molecule can adsorb or attach. Once the molecule of SO is adsorbed onto the catalyst surface, the catalyst can facilitate the activation of chemical bonds, including the oxygen-carbon (O-C) bonds. As agreed with Dawes et al. [83], this chemical bond activation lowers the energy barrier for breaking these bonds as a result of the high green diesel produced. Furthermore, as reported by Hafriz et al. [84], The CDO process exhibits superior efficiency and selectivity compared to thermal deoxygenation. This enables the reaction to take place under mild conditions while optimizing the generation of green diesel and reducing the creation of undesired by-products and impurities. In thermal cracking, the lack of
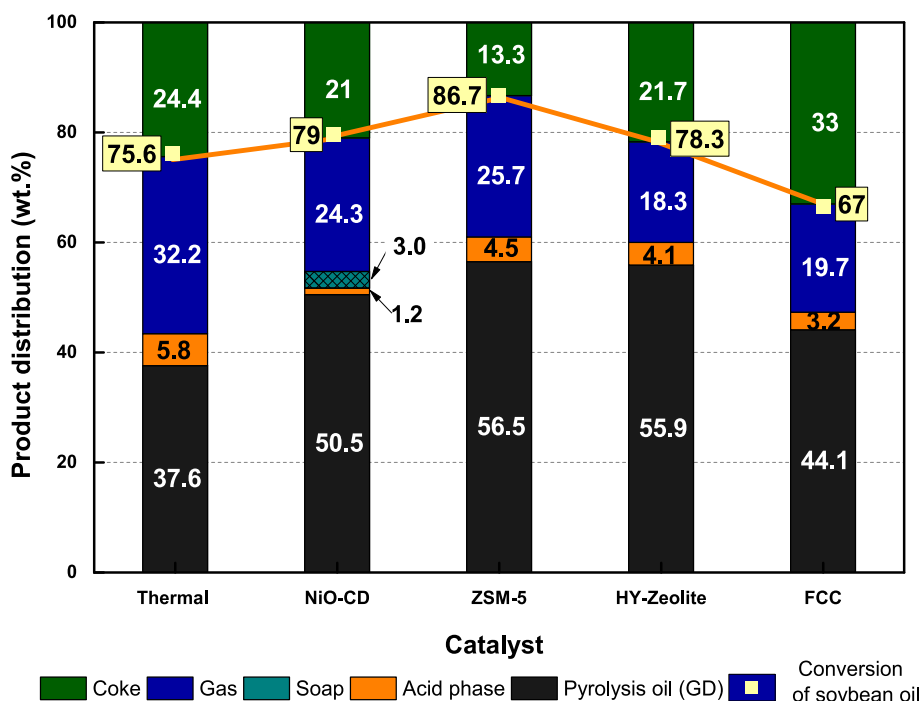

Fig. 5. Product distribution of CDO of SO using various catalysts used.

selectivity can lead to a mixture of products, including impurities and yield high formation of gases (lighter). This discovery was consistent with the result depicted in Fig. 5 under thermal reaction, the formation of gas as a by-product was slightly elevated as compared to the other CDO using NiO-CD and commercial zeolite-based catalyst. The thermal reaction without a catalyst presented a low yield of green diesel (37.6 wt %), which highlights the significance of catalysts in the CDO process of SO. Besides that, the insignificant formation of soap can be observed utilizing the NiO-CD catalyst, which is attributed to the catalyst's high density of basic sites and strong basic strength distribution. As reported by a previous study, the soap formation occurred by the reaction of carboxylic acid (RCOOH) in the feedstock with Calcium Carbonate (CaCO$_3$), using a Ni/CMD900 catalyst with high basic strength (T$_{max}$ = 822 °C) and basic density (7306.37 μmol/g) [39]. The CaCO$_3$ could be formed due to the absorption of in situ CO$_2$ by CaO, and in situ CO$_2$ was generated due to the decarboxylation reaction of oxygenated compounds of SO to produce saturated hydrocarbon alkane compounds. The formation of coke was higher using FCC catalyst followed by thermal > HY-zeolite > NiO-CD > ZSM-5. As reported by Di Vito et al. [5], another potential consequence of coke formation involves the polymerization of alkanes or aromatic compounds, resulting in the creation of a carbonaceous residue composed of dense hydrocarbons. The presence of this coke significantly inhibits the catalyst's activity by adsorbing onto it and obstructing its pores. Besides that, based on Fig. 5, a small formation of acid phase as a by-product can be clearly observed in the lower phase of the resulting liquid product produced. As discovered by Hafriz et al. [44], the acid phase in the form of water has been generated due to the decarbonylation of oxygenates compounds by releasing CO gas and the acid phase contains a significant concentration of carboxylic acid compounds, as shown by GC–MS analysis. Fig. 6 shows the colour of liquid products produced using various catalysts. The dark brown colour of a liquid product can be observed using the NiO-CD catalyst and the dark greenish colour while using ZSM-5 and HY-Zeolite catalyst. The yellowish colour of the liquid product has been produced using an FCC catalyst and two phases of the liquid product can be clearly observed and separated; the upper layer was a green diesel while the bottom layer was an acid phase. The colour of green diesel can also be influenced by any remaining impurities or contaminants present in green diesel that may not have been completely removed during the production process.

Chemical composition of green diesel

Fig. 7 displays the distribution of hydrocarbon and oxygenated compounds in the green diesel produced through CDO using different catalysts. The hydrocarbon and oxygenated compound produced was assessed using GC–MS analysis. NiO-CD catalyst shows tremendous results in yielding 88.63 % of hydrocarbon compounds by lowering the amount of oxygenated compounds to 11.37 % with 88.6 % efficiency of oxygenated compound removal in green diesel composition produced as compared to other catalysts. The existence of the synergistic effect of NiO and CaO/MgO in the NiO-CD catalyst is likely responsible for this phenomenon, which removes oxygen molecules by absorption of CO$_2$ in the gas phase. Thus, it slightly affects the hydrocarbon composition and quality of green diesel produced, as shown in Fig. 7. Lower oxygen content in green diesel is generally preferred because oxygen content can impact the energy content of the biofuel and its stability when stored. As reported by Sundus et al. [85], the increase of oxygen in fuel structure results in a reduction of hydrocarbon composition in the fuel resulting in lower energy content and lower oxidation stability in a high-heating environment compared to petroleum-based fuels. The presence of oxygen in the form of different aliphatic and aromatic oxygenates will have an impact on the quality of bio-oil, as indicated by earlier studies. Hence, it is imperative to decrease the overall quantity of oxygenated chemicals in the green diesel generated through CDO. The application of commercial zeolite-based catalysts led to a modest increase in the overall amount of oxygenated molecules. Besides that, the modification of the porous structure of the NiO-CD catalyst from macroporosity to mesoporosity structure due to the successful NiO dispersion on to dolomite support catalyst and improvement of surface area produce a better route efficiently for eliminating oxygen in the form of CO$_2$ using CDO reaction. This discovery was consistent with the study reported by Ooi et al. [61], the mesoporous structure and large surface area of synthesized Al$_2$O$_3$-TiO$_2$ catalyst facilitates rapid diffusion of triolein, hence enhancing its catalytic efficacy. In this work, it has been shown that zeolites, although commonly recognised for their high catalytic activity in cracking processes because of their solid acid properties, exhibit reduced activity compared to thermal cracking (without a catalyst). However, the production yield of green diesel utilising the zeolite catalyst exceeds that achieved by thermal cracking (Fig. 5). Additionally, the oxygenated compounds present in the product from the Zeolite catalyst are greater than those from the thermal cracking, especially when using ZSM-5 and HY catalysts, as shown in Fig. 7. However, both are lower than those found in products produced using a modified dolomite catalyst. This trend was apparent in prior work [26], where the thermal cracking reaction yielded just a small amount of green diesel but a higher percentage of hydrocarbons (low-oxygenated compounds)

Fig. 6. The colour of liquid products produced using various catalysts.
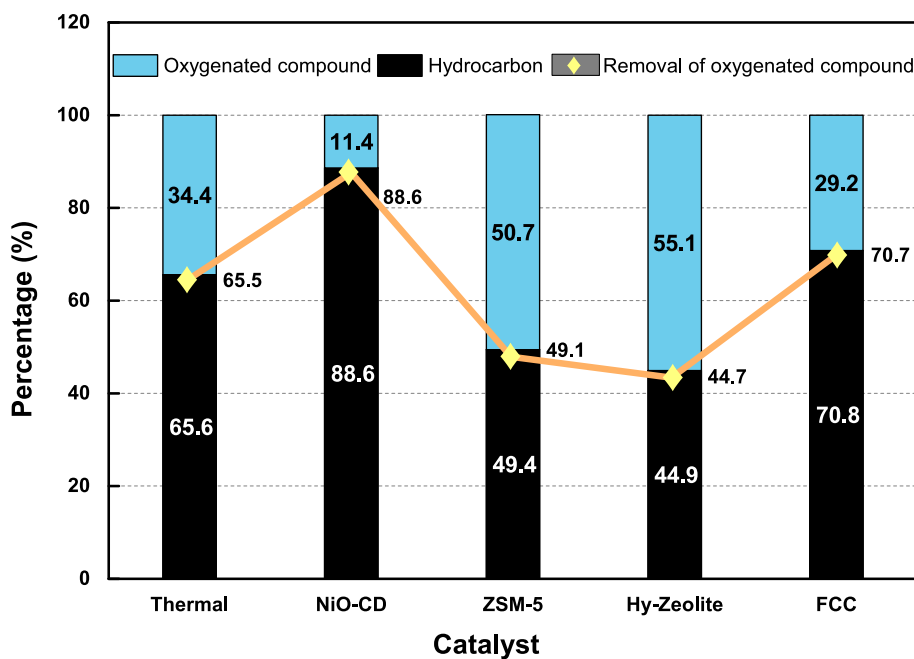
Fig. 7. The composition of green diesel under various catalysts used. (For interpretation of the references to colour in this figure legend, the reader is referred to the web version of this article.)

compared to commercial zeolite catalysts in the catalytic deoxygenation of waste cooking oil. Thermal cracking (without catalyst) produced 1.73 wt% of green diesel, accompanied by a minimal quantity of oxygenated compounds (35.73 %), in contrast to ZSM-5 (48.01 %), HY-zeolite (48.06 %), and FCC (51.3 %). Nevertheless, the yield of green diesel produced with these commercial zeolite catalysts exceeded 10 wt%. Zeolites, including their microporous structure and high acidity, are often very efficient in facilitating hydrocarbon cracking, resulting in the decomposition of long-chain hydrocarbons into smaller, more economically valuable molecules. Nevertheless, the reduced deoxygenation activity observed through amount of oxygenated compound in this investigation compared to thermal cracking could be attributed to the potential influence of coke production. A carbonaceous residue, known as coke, can accumulate on the surface of zeolite during reactions, obstructing active sites and diminishing catalytic effectiveness. Consequently, the zeolite's capacity to maintain a high rate of cracking activity decreases over time. Moreover, in this study, the reaction conditions may not have been completely optimised for the zeolite, resulting in less activity than thermal cracking, which could occur more vigorously at specific temperatures without the catalyst. As observed in Fig. 7, commercial zeolite-based catalysed pyrolysis tends to favour pathways that introduce or retain oxygen in the product molecules, contributing to the higher oxygenated compound content in the green diesel produced from SO. Commercial acid zeolite-based catalysts in CDO of SO may lead to the formation of high-oxygenated compounds, which could be due to the acidic environment facilitating the cleavage of chemical bonds (cracking process), leading to the formation of smaller fragments. The cracking process can generate oxygenated compounds as by-products, such as carboxylic acids, ketones and aldehydes, which can be observed clearly in Table 5. Besides that, these acidic conditions can lead to the self-hydrolysis of esters and other oxygenated functional groups present in the presence of SO at a reaction temperature of 100 – 240 °C. This reaction has been proved to occur as reported by Asikin Mijan *et al.* [46], when the triacylglycerides in Jatropha curcas oil will undergo initial decomposition into its fatty acids through the cleavage of C-O bonds via self-hydrolysis of the ester. The presence of acidic sites facilitates the breaking of ester linkages, releasing fatty acids and contributing to the oxygenated content of the resulting green diesel.

Table 5
Composition profile of hydrocarbon and oxygenated compound in green diesel.

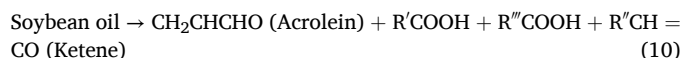| Compositions (%)	Thermal	NiO-CD	ZSM-5	HY-Zeolite	FCC
Hydrocarbon compound					
Alkanes	22.72	28.58	10.73	15.48	18.20
Alkenes	26.78	42.77	24.57	21.58	23.81
Diene	1.40	0.86	0.37	0.00	0.53
Alkyne	0.92	4.04	1.55	0.00	1.20
Cycloalkane	7.55	5.49	5.69	4.97	8.25
Cycloalkene	3.03	3.58	2.50	1.66	4.97
Aromatic	3.20	3.31	3.94	1.21	13.81
Oxygenated compound					
Ester	0.23	0.23	0.37	0.45	0.00
Carboxylic Acid	15.46	0.00	34.14	33.49	17.09
Ketone	4.39	5.36	5.71	3.77	3.08
Alcohol	9.93	3.53	8.47	15.87	6.66
Others	4.39	2.25	1.96	1.52	2.40

The composition of hydrocarbon and oxygenated in green diesel produced using different catalysts was summarised in Table 5. The hydrocarbon composition was determined and classified in the carbon range of 8 to 24 using GC–MS analysis. The major hydrocarbon composition presence in green diesel is alkenes and alkanes, followed by cycloalkanes, aromatic cycloalkanes, alkynes, and dienes. It aligned with the study undertaken by Al-sultan *et al.* [45], the major compound presence in the deoxygenated liquid produced via catalytic deoxygenation of WCO using the CaO-La$_2$O$_3$/AC catalyst consisted of straight chain hydrocarbons containing both saturated and unsaturated compounds. In this study, the NiO-CD catalyst yielded a high amount of alkanes and alkenes due to the synergistic effect of NiO and CaO/MgO presence in the NiO-CD catalyst, creating bifunctional acid-base properties. The NiO-CD catalyst exhibits bifunctional acid-base properties due to the complementary nature of dolomite catalyst support that attributes more to the base properties, while Nickel carries the acidic properties [86]. The incorporation of NiO onto the CaO and MgO-rich dolomite support generates a multicomponent active site environment that facilitates simultaneous and efficient catalytic reactions. Besides that, the successful dispersion of NiO onto Malaysian dolomite support

catalyst will contribute to participating in hydrogen transfer reactions. These hydrocracking processes frequently involve introducing in situ hydrogen to cleave carbon–carbon bonds found in the fatty acid content of SO. The nickel species on the NiO-CD catalyst can facilitate the transfer of in situ hydrogen to unsaturated bonds, leading to the saturation of double bonds and the transformation of complex hydrocarbons into lighter products. As observed in Table 5, there are significant changes between thermal and CDO using NiO-CD catalyst where the production of alkanes and alkenes has been increased. This could be attributed to the secondary reactions occurring on the active site of the catalyst, particularly the deoxygenation reaction pathways. However, as compared to commercial zeolite-based catalysts in CDO, the composition of alkanes and alkenes was decreased due to the high formation of deoxygenated compounds. As reported by Yu et al. [57], alkanes are preferred for their stability and low reactivity compared to alkenes. This is because alkenes have a negative impact on the stability of oil oxidation and the long-term storage of alkenes often leads to the formation of gum deposits. Consequently, the long-term storage of alkenes typically necessitates the application of antioxidants. The formation of cycloalkanes and cycloalkenes has been observed in Table 5 with the presence of a small formation of aromatic, dienes and alkynes. Based on the previous study [21], the alkenes underwent a Diels-Alder reaction, resulting in the formation of cycloalkenes. This chemical serves as the primary hydrocarbon for synthesizing the cyclic and aromatic hydrocarbons found in green diesel. While cycloalkanes are formed through the process of hydrogenation, when hydrogen is removed from cycloalkenes through abstraction. This process directly contributes to the stabilization of radicals. The presence of a high amount of aromatic compound has been observed at 13.81 % while using FCC. Based on Worldwide Fuel Charters [87], the combusting of aromatic compounds can result in the production of carcinogenic benzene in exhaust gases and the accumulation of combustion chamber deposits, leading to elevated levels of tailpipe emissions. The reduction of aromatic levels in gasoline has a substantial impact on the decrease of harmful benzene emissions in vehicle exhaust, as demonstrated in both the US AQIRP and the European EPEFE investigations. Nevertheless, the substantial concentration of aromatic compounds in green diesel can significantly influence its characteristics, including density and cloud point.
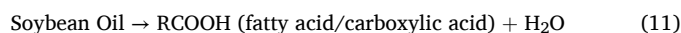
The main oxygenated composition of green diesel is mainly comprised of carboxylic acid and alcohol as presented in Table 5. As discovered by Fahim et al. [88] and Hafriz et al. [26], the presence of alcohols, ethers, carboxylic acids, phenolic compounds, ketones, esters, and anhydrides with a high oxygen concentration suggests that the oil has been exposed to the atmosphere for an extended period of time. The existence of oxygenated compounds leads to the oil being acidic, which in turn results in processing issues such as corrosion, cold filter clogging point, and freezing point of the oil. The presence of a mesoporous structure in the NiO-CD catalyst facilitates the conversion of carboxylic acid in SO into hydrocarbon. This is achieved by effectively removing oxygen through the release of CO_2, CO, and H_2O molecules via an efficient deoxygenation pathway as compared with other catalysts (Table 5). Eq. (10)–(15) shows the possible reaction to produce an oxygenated compound as observed in green diesel. The initial decomposition or under thermal cracking of SO (triglyceride) produced fatty acid/carboxylic acid, acrolein and ketenes (Eq. (10)). Based on a study conducted by Idem et al. [89], the initial decomposition or thermal cracking of triglyceride will yield heavy oxygenated hydrocarbons, including long-chain fatty acids (carboxylic acid, RCOOH), ketones (R'COR''), aldehydes (RCHO), and esters (RCOOR'). Besides that, the triglyceride of SO will undergo self-hydrolysis as a result of the existence of air or oxygen to generate carboxylic acid and water as by-products as mentioned in Eq. (11). It was in line with a study discovered by Aliana et al. [90] and Idem et al. [89], that the triglyceride of chicken fat oil (CFO) and canola oil initially undergone self-hydrolysis under catalytic deoxygenation reaction and thermal cracking reaction, respectively. While the formation of the ketone compound has been produced via the

ketonization reaction of two carboxylic acids by releasing water and carbon dioxide as mentioned in Eq. (12). This reaction can be clearly observed in the ketonization of a mix of valeric acid and pivalic acid with the presence of an acid catalyst for bio-oil upgrading via catalytic pyrolysis conducted by Pham et al. [91]. While the small formation of aldehydes could be observed in the dehydration reaction of carboxylic acid with the presence of in situ hydrogen and the formation of water as a by-product (Eq. (13)). The in-situ hydrogen was produced as a result of the Water-gas shift reaction in the catalytic deoxygenation process [84]. In CDO of SO, hydrogenation of aldehyde (Eq. (14)) with the presence of in situ hydrogen could occur for producing alcohol which is a compound that is present in the green diesel composition as tabulated in Table 5. These two reactions were in agreement with Altalhi et al. [92] whereas two probable pathways for stearic acid have been identified: the first involves the dehydration of stearic acid to become octadecanal (an aldehyde), which is then transformed to octadecanol (the equivalent alcohol) by a hydrogenation reaction. The hydrogenation of ketones was the second possible reaction due to the presence of in situ hydrogen which yielded intermediate oxygenation of alcohol as mentioned in Eq. (15).

1. Initial decomposition/cracking of triglyceride

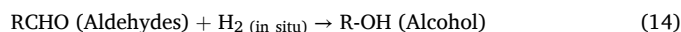$$\text{Soybean oil} \rightarrow CH_2CHCHO \text{ (Acrolein)} + R'COOH + R'''COOH + R''CH = CO \text{ (Ketene)} \qquad (10)$$

2. Hydrolysis

$$\text{Soybean Oil} \rightarrow RCOOH \text{ (fatty acid/carboxylic acid)} + H_2O \qquad (11)$$

3. Ketonization

$$R'COOH + R''COOH \rightarrow R'COR'' \text{(Ketones)} + H_2O + CO_2 \qquad (12)$$

4. Dehydration

$$RCOOH + H_{2 \text{ (in situ)}} \rightarrow RCHO \text{ (Aldehydes)} + H_2O \qquad (13)$$

5. Hydrogenation

$$RCHO \text{ (Aldehydes)} + H_{2 \text{ (in situ)}} \rightarrow R\text{-}OH \text{ (Alcohol)} \qquad (14)$$

$$R'COR'' \text{ (Ketones)} + H_{2 \text{ (in situ)}} \rightarrow R'CHOHR'' \text{(Alcohol)} \qquad (15)$$

The hydrocarbon compound present in green diesel has been identified using GC–MS analysis with the carbon number range of 8 to 24, as tabulated in Fig. 8(a). The formation of hydrocarbon with carbon number range of C_8 and C_{14} could be observed in green diesel composition as a result of carbon loss through the process of carboxylic acid cracking light straight chain hydrocarbons are formed as shown in Table 6(a). In Fig. 8(a), the synergistic effect of NiO and CaO/MgO phase exhibits bi-functional acid-base characteristics once NiO is successfully dispersed onto the dolomite support, showing an improvement in cracking reaction of C-C bond due to the high yielded of hydrocarbon range C_8-C_{14} as compared to the thermal cracking. In CDO using NiO-CD catalyst, predominant hydrocarbon products are found in the C_{15} and C_{17} fractions due to the decarboxylation/decarbonylation (deCOx) reaction being the dominant process. We can clearly observe that these fractions were associated with the composition of SO feedstock which comprises long-chain fatty acids of C_{16} (palmitic acid) and C_{18} (oleic acid and stearic acid). As mentioned by Pimenta et al. [93] and Baharuddin et al. [94], the deCOx pathways result in the synthesis of a hydrocarbon that has one fewer carbon atom compared to the initial fatty acid. The strong preference for C_{15} and C_{17} indicates that the deCOx reaction pathways are favoured due to the production of CO_2, CO, and H_2O as by-products. It shows that the mesoporosity structure of NiO-CD catalyst could improve and provide more pathways for deCOx reaction to occur by removing oxygen content and yielding high hydrocarbon compounds in green diesel. Based on Fig. 8(a), a hydrocarbon with a number range of C_{16} and C_{18} with an equal amount of carbon atoms as the initial fatty acid can be observed in green diesel composition after
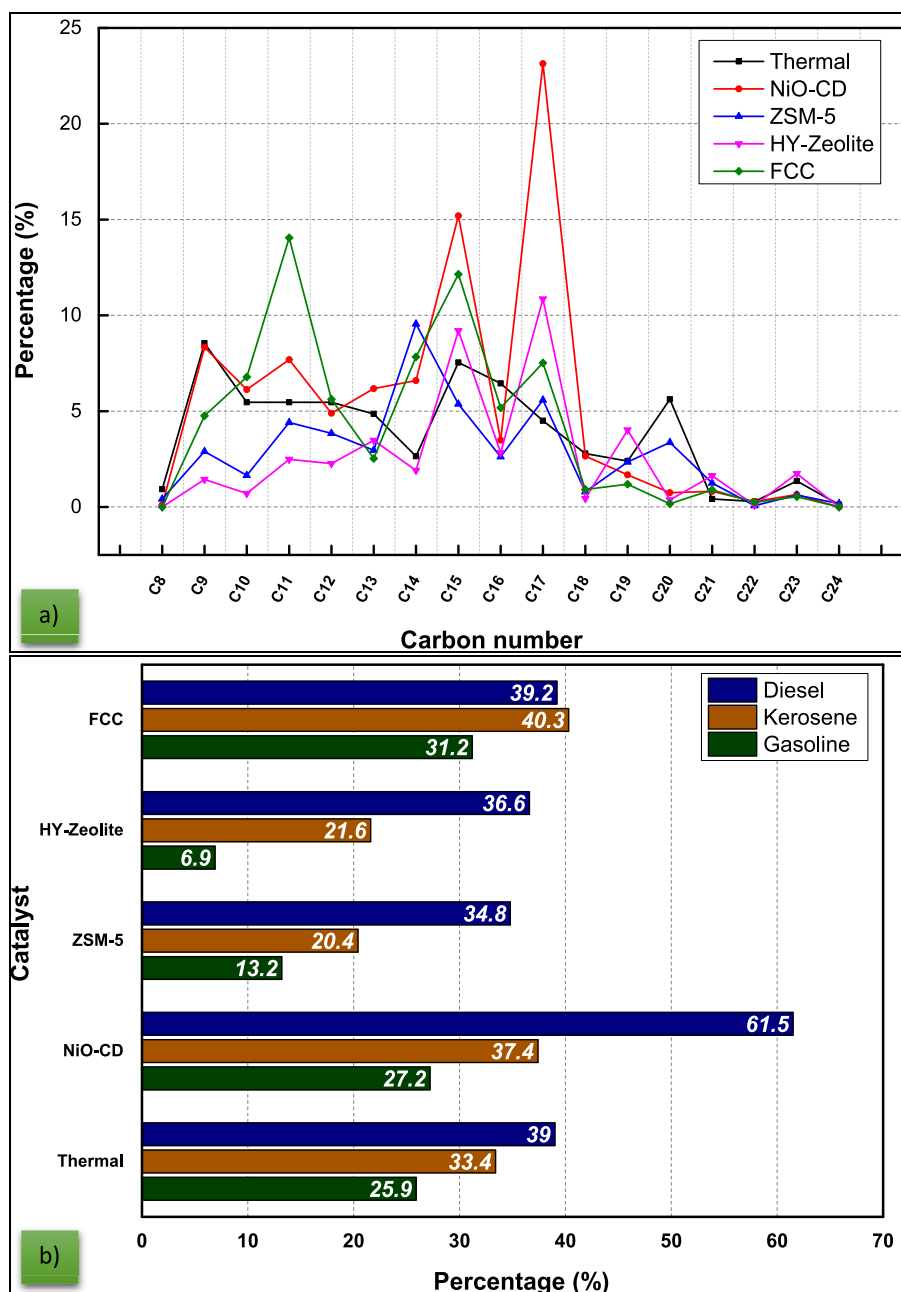
Fig. 8. A) Product selectivity based on carbon number of hydrocarbon and b) selectivity towards gasoline, kerosene and diesel range fuel.

undergoing hydrogenation (HDO) of fatty acid. As reported by Pimenta *et al.* [93], the HDO pathway utilises a NiMo carbide-based catalyst to generate a hydrocarbon that possesses an equivalent number of carbons as the initial fatty acid found in soybean oil.

Fig. 8(b) reveals all the catalyst and thermal deoxygenation yielded hydrocarbon compounds with selectivity towards diesel range fuel except FCC catalyst. Based on the previous study [44], the gasoline range is categorised based on hydrocarbons with carbon numbers ranging from C_8 to C_{12}. Diesel, on the other hand, consists of hydrocarbons with carbon numbers ranging from C_{13} to C_{24}. Kerosene is defined as a blend of saturated hydrocarbons, including alkanes, cycloalkanes, and aromatic components, with carbon numbers ranging from C_8 to C_{24}. As mentioned by Basir *et al.* [64] and Caceres-Martinez *et al.* [95], typically, commercial jet fuel or kerosene range fuel consists of three main components hydrocarbon, including alkanes, cyclic alkanes and aromatic hydrocarbons. The improvement of the porous structure of

NiO-CD catalyst to mesoporous structure provides the efficiency of conversion SO into green diesel with tremendous results in yielding high saturated and unsaturated hydrocarbon (84.6 %) and producing the highest selectivity of diesel fuel fraction (61.5 %) as compared to others catalyst. However, FCC shows the selectivity towards kerosene range fuel, which contains saturated hydrocarbon. This could be due to the high pore volume of FCC catalyst which provides better diffusion space for long chain hydrocarbon for further cracking into shorter carbon chain of C_9-C_{12} which is in line with the dominant formation of hydrocarbon range of C_9-C_{12} exists in green diesel as illustrated in Fig. 8(b). The investigation successfully examined the production of green diesel using CDO of SO, employing several catalysts. The NiO-CD catalyst was chosen as the most effective deoxygenation catalyst due to its remarkable capacity to remove oxygen content. This is crucial for ensuring the excellent quality of the green diesel generated, particularly in terms of its physical and chemical qualities.

Table 6
Composition profile of hydrocarbon and oxygenated compound in green diesel.

Compositions (%)	1 wt%	3 wt%	5 wt%	7 wt%
Hydrocarbon compound				
Alkanes	32.10	22.04	28.58	21.16
Alkenes	35.35	44.97	42.77	34.83
Diene	1.27	1.68	0.86	2.42
Alkyne	1.36	2.45	4.04	1.99
Cycloalkane	5.24	4.49	5.49	9.57
Cycloalkene	3.02	3.50	3.58	2.98
Aromatic	2.12	2.68	3.31	10.98
Oxygenated compound				
Ester	0.00	1.23	0.23	1.08
Carboxylic Acid	1.92	0.86	0.00	0.00
Ketone	2.58	5.20	5.36	6.74
Alcohol	10.58	6.54	3.53	4.75
Others	4.46	4.36	2.25	3.50

Effect of NiO-CD catalyst loading

Product distribution using mass balance

Fig. 9 demonstrates the impact of varying percentages of NiO-CD catalyst loading on the distribution of products and the conversion rates of SO into green diesel. The study has been conducted via CDO of SO at a reaction temperature of 400 °C ± 10 °C for 30 min and 50 cm^3/ min of continuous nitrogen flow which is required to maintain an oxygen-depleted condition within the system. As shown in Fig. 9, catalyst loading affects the product distribution via CDO, especially in terms of yield of green diesel and SO conversion. The increasing catalyst loading will enhance the conversion of SO to liquid and gas products due to the presence of a more active site. When there is an excessive amount of catalyst loading in the reaction, the reactant has a larger contact surface, which increases the reaction activity during the CDO of SO. At a higher amount of catalyst loading, SO will be easily cracked into gas and will increase the possibility of condensing as a liquid product and at the same time reduce the coke formation. It was clearly observed at 7 wt% of catalyst loading with high formation of gas product (34.9 wt%). As

reported by Asikin Mijan *et al.* [46], increasing the catalyst loading led to a heightened thermal cracking efficiency, resulting in the production of shorter hydrocarbon fractions, namely gaseous products. At elevated temperatures, the process of thermal cracking will lead to the production of additional volatile substances and a decrease in output. Nevertheless, the production of green diesel at a catalyst loading of 7 wt% resulted in a decreased yield of 44.6 wt%, mostly due to the significant development of soap (3.98 wt%) and acid phase (1.86 wt%), in comparison to other catalyst loadings. The existence of catalyst loading will create more calcium carbonate (after reacting with in situ CO$_2$) which reacts with the carboxylic acid of feedstock to form soap and it will slightly reduce the yield of green diesel. As discovered by Kwon *et al.* [96], using an excessive amount of catalyst increases the possibility of secondary reactions, which include the polymerization and cracking of dense oxygenated compounds. Polymerization processes provide substantial products, including sizable aromatic by-products and asphaltenes, which pose harm to the catalyst surface and thus lead to catalyst deactivation. At a catalyst loading of 5 wt%, the availability of active sites for deoxygenation and cracking reactions will be enhanced, resulting in an increased yield of green diesel. This discovery was consistent with the investigation conducted by Obeas *et al.* [97], at catalyst loading of 5 % of 15 % Co - 25 % La supported activated catalyst, there is a notable improvement in yield. Specifically, 80 % of the green diesel produced from the deoxygenation of Jatropha oil is achieved using free hydrogen and solvent. Increasing the catalyst loading to 7 wt % results in a decrease in the yield to 22 %. Exceeding the optimal amount of catalyst will enhance the occurrence of secondary and parallel reactions due to the surplus of active sites available for multiple reactions. Consequently, the production of green diesel will decrease beyond a catalyst loading of 5 wt%. The colour of green diesel, produced through CDO of SO with varying catalyst loading percentages, is seen in Fig. 10. The green diesel exhibits a brown colour when employing catalyst loadings of 1 and 3 wt% of NiO-CD, and a transparent brown colour when applying a catalyst loading of 5 wt% of NiO-CD. However, at a high amount of catalyst loading, the colour of the green diesel produced will be darker, which could be due to the formation of ketones, as shown in Table 6. The formation of ketones, a type of organic compound with a carbonyl group bonded to two carbon atoms, can
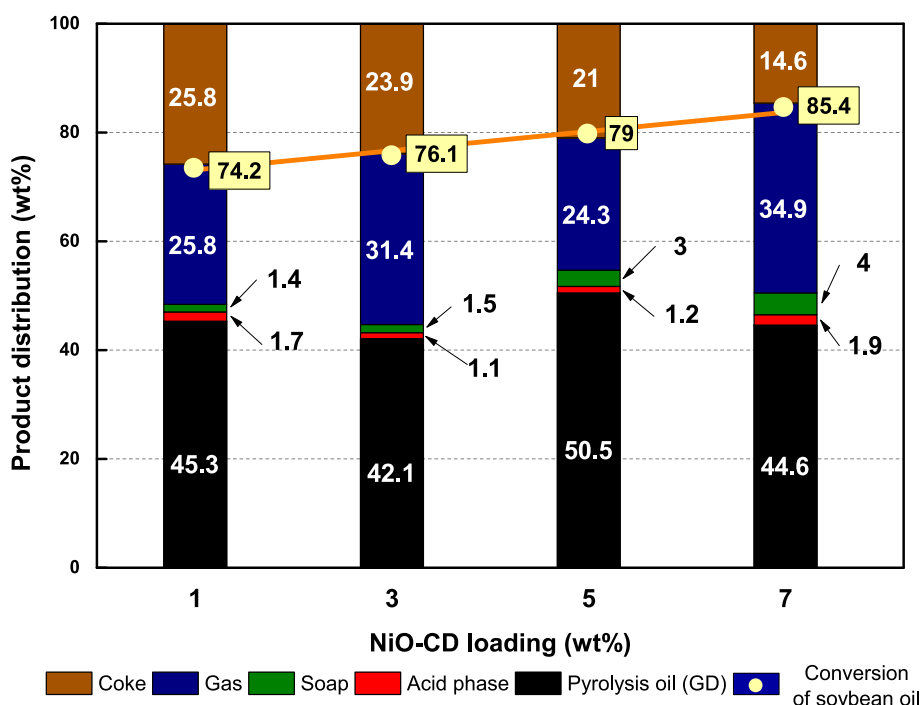

Fig. 9. Product distribution of CDO of SO using various catalyst loading.

Fig. 10. Colour of green diesel produced at various amount of catalyst loading. (For interpretation of the references to colour in this figure legend, the reader is referred to the web version of this article.)

contribute to colour changes. However, the colour of green diesel can also be affected by any remaining impurities or contaminants in green diesel that were not completely removed during the process. These impurities tend to have a strong rancid smell of green diesel produced. As discovered by Malvarinda et al.[98], as the amount of catalyst in the catalytic hydrogenation of palm fatty acid distillate increases, the colour of the produced green diesel becomes more intense and the smell becomes slightly rotten. This is attributed to the production of residue and contaminants.

Chemical composition of green diesel

The potential of NiO-CD as a deoxygenation catalyst by removing oxygenated compounds in the final product of green diesel using different percentages of catalyst loading is evaluated and the results are displayed in Fig. 11. Based on Fig. 11, the different percentages of NiO-CD catalyst loading will generate different yields of hydrocarbon compounds. However, the yield of hydrocarbon compounds for different catalyst loading was more than > 80 %. With a higher catalyst loading, the quantity of oxygenated molecules decreases, likely because of the substantial active site of NiO-CaO/MgO. This active site facilitates the

removal of oxygen by efficiently absorbing more CO_2 in the gas phase. Consequently, the hydrocarbon composition in green diesel was slightly influenced, as seen in Table 6. CaO and MgO presence enhances the efficacy of CDO, resulting in more efficient removal of oxygen in the form of CO_2 and CO. The total quantity of oxygenated compounds dropped slightly as a result of applying the higher amount of catalyst loading; however, at 7 wt% of catalyst loading, the oxygenation started to increase while the hydrocarbon composition was reduced. This reduction could be due to a variety of factors, including over-reaction, side effects, or a shift in the process's selectivity towards undesirable products, as shown in Table 6. In a chemical reaction, the catalyst facilitates the reaction but is not consumed in the process. Excess catalysts can sometimes improve reaction rate, but it can also have negative consequences such as increased costs and potential effects on the final product. Based on previous studies [26], the presence of various aliphatic and aromatic oxygenates will have an impact on the quality of green diesel. Biofuel, despite its elevated oxygen content, is not a viable alternative to petrol diesel due to its high corrosiveness, storage instability, and limited compatibility with traditional fossil fuels [99]. Besides that, a higher oxygen level will lead to a decrease in the calorific value, energy density, and energy content [100]. Therefore, the total oxygenated compounds in the bio-oil must be reduced and catalyst loading at 5 wt% was the optimal loading for deoxygenation reaction. Overall, it was determined that an increased amount of catalyst resulted in higher triglyceride C-C scissions and degradation into intermediate products, specifically carboxylic acid groups. There was a lower incidence of C-O scission through the deCOx reaction. These findings indicate that a higher catalyst loading is not desirable for the deCOx reaction.

The hydrocarbon composition of green diesel primarily consists of straight-chain alkanes and alkenes, as seen in Table 6. During the deoxygenation of carboxylic acid, the formation of alkenes was accomplished through the elimination of carbon monoxide (CO) and water (H_2O) molecules via a decarbonylation reaction (Eq. (16)), dehydrogenation of alkanes (Eq. (17)) [82] and dehydration of alcohol (Eq. (18)) [92]. Meanwhile, the increase in straight alkane's formation possibly took place after the release of the CO_2 group from the SO via decarboxylation reaction (Eq. (19)), decarbonylation of aldehyde/
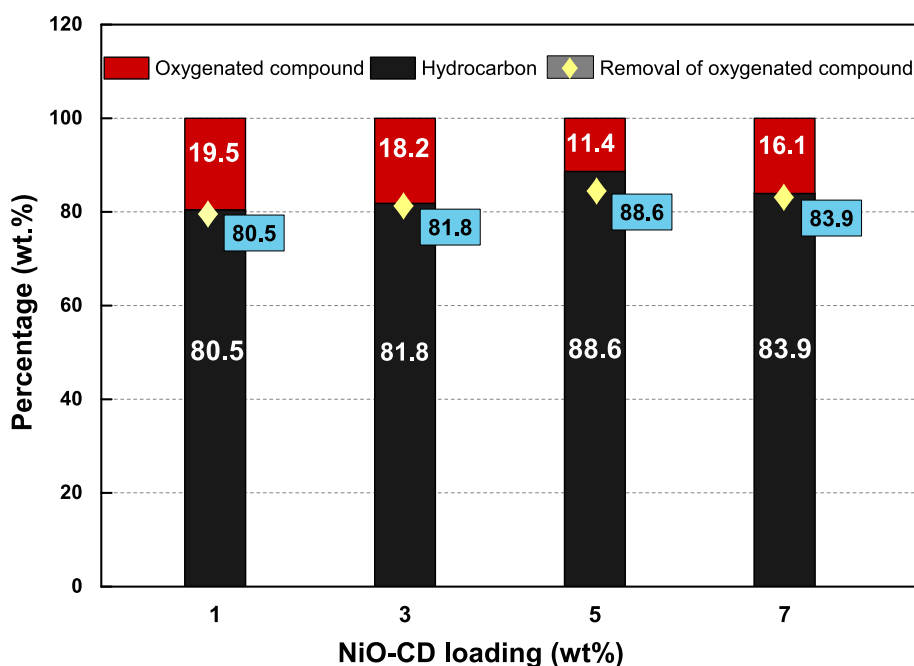
Fig. 11. The composition of green diesel under various amounts of catalyst loading. (For interpretation of the references to colour in this figure legend, the reader is referred to the web version of this article.)
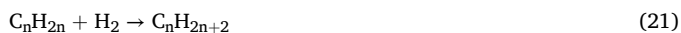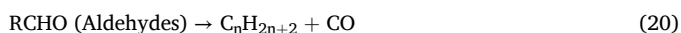
ketones (Eq. (20)), hydrogenation of alkenes (Eq. (21)) [33] and oligomerization of light alkenes to produce heavier alkanes via structural modification (Eq. (22)) [101]. The increasing hydrocarbon mixture of alkanes and alkenes can be observed in 5 wt% catalyst loading (71.35 %) followed by 1 wt% (67.45 %) > 3 wt% (67.01 %) and 7 wt% (55.99 %).

Equation

Alkenes formation

$$RCOOH \rightarrow C_nH_{2n} + CO + H_2O \tag{16}$$

$$C_nH_{2n+2} \rightarrow C_nH_{2n} + H_2 \tag{17}$$

$$R\text{-}OH \rightarrow C_nH_{2n} + H_2O \tag{18}$$

Alkanes formation

$$RCOOH \rightarrow C_nH_{2n+2} + CO_2 \tag{19}$$

$$RCHO \text{ (Aldehydes)} \rightarrow C_nH_{2n+2} + CO \tag{20}$$

$$C_nH_{2n} + H_2 \rightarrow C_nH_{2n+2} \tag{21}$$

$$C_nH_{2n} \rightarrow C_nH_{2n+2} \text{ (Heavier)} \tag{22}$$

As reported by Caceres-Martinez *et al.* [95], like other hydrocarbons, cycloalkanes have a high energy density. This means that green diesel containing cycloalkanes has a high energy density per unit volume when compared to n-alkanes, isoalkanes and aromatic compounds, making it an efficient fuel. Furthermore, cycloalkanes have lower boiling points than alkanes. As mentioned in Fig. 12, the cycloalkenes were generated due to the reaction between a conjugated diene and an alkene (Eq. (23)). At 7 wt% of catalyst loading, the cycloalkane was highly produced (9.57 %) via hydrogenation of cycloalkenes (Eq. (24)) utilising in situ hydrogen derived from the water–gas shift reaction. This reaction possibly occurred due to the reduction of cycloalkenes compound presence in green diesel reaction as compared to other catalyst loading. Besides that, this reduction compound can occur due to the high formation of the aromatic compounds through the dehydrogenation of cycloalkenes (Eq. (25)) [21]. The presence of a high amount of aromatic compound has been observed with 7 wt% of catalyst loading. It was

consistent with the study conducted by Asikin Mijan *et al.* [46], which found that higher catalyst loading of more than 5 wt% has led to a reduction in hydrocarbon production due to the potential occurrence of parallel or secondary reactions. Consequently, the elevated catalyst loading will result in the carcinogenic impact of aromatic compounds in fuels, which is the focus of the 'European initiative on emission fuels and engine technologies' aiming to decrease the benzene level in gasoline [87,102].

As observed in Table 6, the increasing amount of catalyst loading will lead to the efficient conversion of carboxylic acid to another compound in green diesel especially at 5 and 7 wt% catalyst loading with 100 % conversion followed by 3 wt% (98.97 %) and 1 wt% (97.70 %). The higher catalyst loading might enhance the rate of the reaction and increase the overall surface area available for the reaction. The increase of catalyst loading can frequently increase the rate of the reaction. This occurs because there are a greater number of active sites on the catalyst surface that are accessible for the adsorption and transformation of reactants. Higher catalyst loading can increase the total available surface area for the reaction and more contact between the reactants and the catalyst surface may result, potentially improving carboxylic acid conversion. Table 6 shows that the amount of catalyst loading will affect the formation of the ketone compound. The increasing of catalyst loading will increase the formation of the ketone via the ketonization reaction of two carboxylic acids, as mentioned in Eq. (13). It possibly occurred due to the reduction of carboxylic acid from 83.63 % of feedstock to less than < 2 % of carboxylic acid in green diesel. The high formation of alcohol compound can be observed with decreasing catalyst loading except at 5 wt% (optimal loading). This shows that the decreasing of the catalyst will favour the hydrogenation of ketones reaction, which yields intermediate oxygenation of alcohol as mentioned in Eq. (15). A prior study has indicated that the acid value of synthesized green diesel is influenced by the presence of oxygenated molecules, particularly carboxylic acid [21]. It was in line as discovered by Shitao *et al.* [103], the presence of carboxylic acid compounds in the composition of biofuel has a substantial influence on the physical properties of the biofuel, including the cold filter clogging point, corrosion value, and freezing point. Hence, it is imperative to develop a novel catalyst that can enhance the quality of liquid hydrocarbon biofuels. In addition, it may be inferred that overloading the catalyst will enhance the possibility of secondary and parallel reactions due to the surplus of active sites
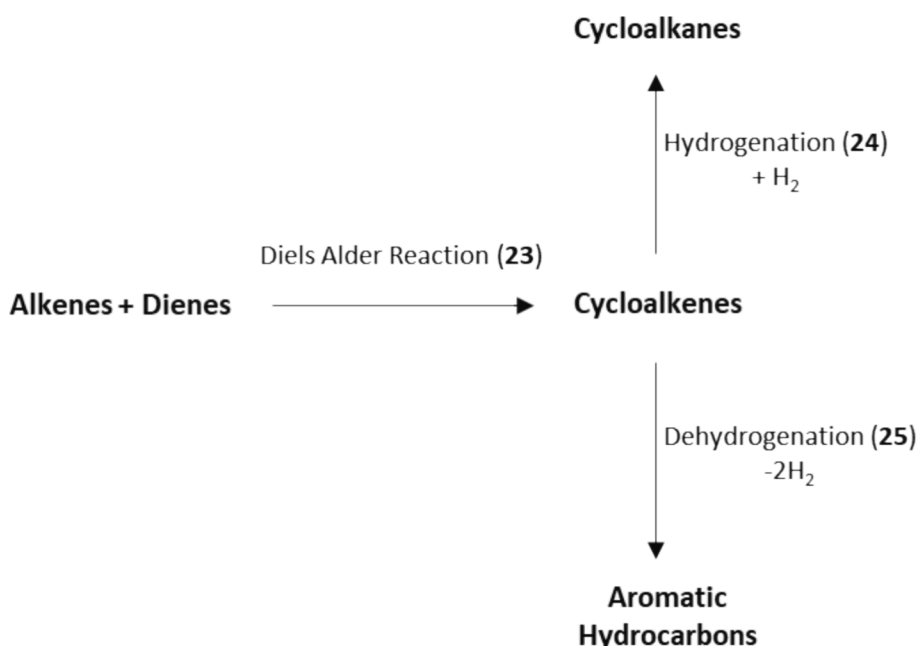

Fig. 12. Reaction involves the formation of cyclic hydrocarbon via deoxygenation.

available for various reactions.

Based on Fig. 13(a), demonstrate the impact of varying quantities of NiO-CD catalyst on the specificity of hydrocarbon (C_8-C_{24}) production under conditions of 400 °C temperature and 30 min reaction time. As observed in Fig. 13(a), at 7 wt% of catalyst loading, the selectivity of hydrocarbon was towards carbon number of C_8 to C_{14} with Σ (C_8-C_{14}) = 50.8 % which shows that the C-C bond cracking reaction was the favourable reaction. Increasing the catalyst loading to 7 wt% led to a decrease in hydrocarbon yield to 83. 8 % and the selectivity of Σ (C_{15} + C_{17}) to 18.9 %. This discovery was consistent with the research conducted by Wan Khalit *et al.* [104], significantly increasing the loading of catalysts with active sites enhances the occurrence of side reactions,

such as C-C cleavage through cracking reaction, and facilitates the production of light hydrocarbons. This finding indicates that 5 wt% catalyst loading was the highest selectivity towards hydrocarbon of Σ (C_{15} + C_{17}) with 38.3 % as compared to other catalyst loading. This indicates that a catalyst loading of 5 wt% NiO-CD was found to be the most effective for promoting deCOx reaction pathways in the CDO of SO. This catalyst loading resulted in the reduction of the carbon chain length by one unit following the removal of CO_2 or CO. The oxygenated compound removal in green diesel can be accomplished through decarbonylation and decarboxylation pathways due to the optimal active site, mesoporosity structure and synergistic effects of NiO and CaO/MgO in creating bi-functional acid-base characteristics of synthesized NiO-CD
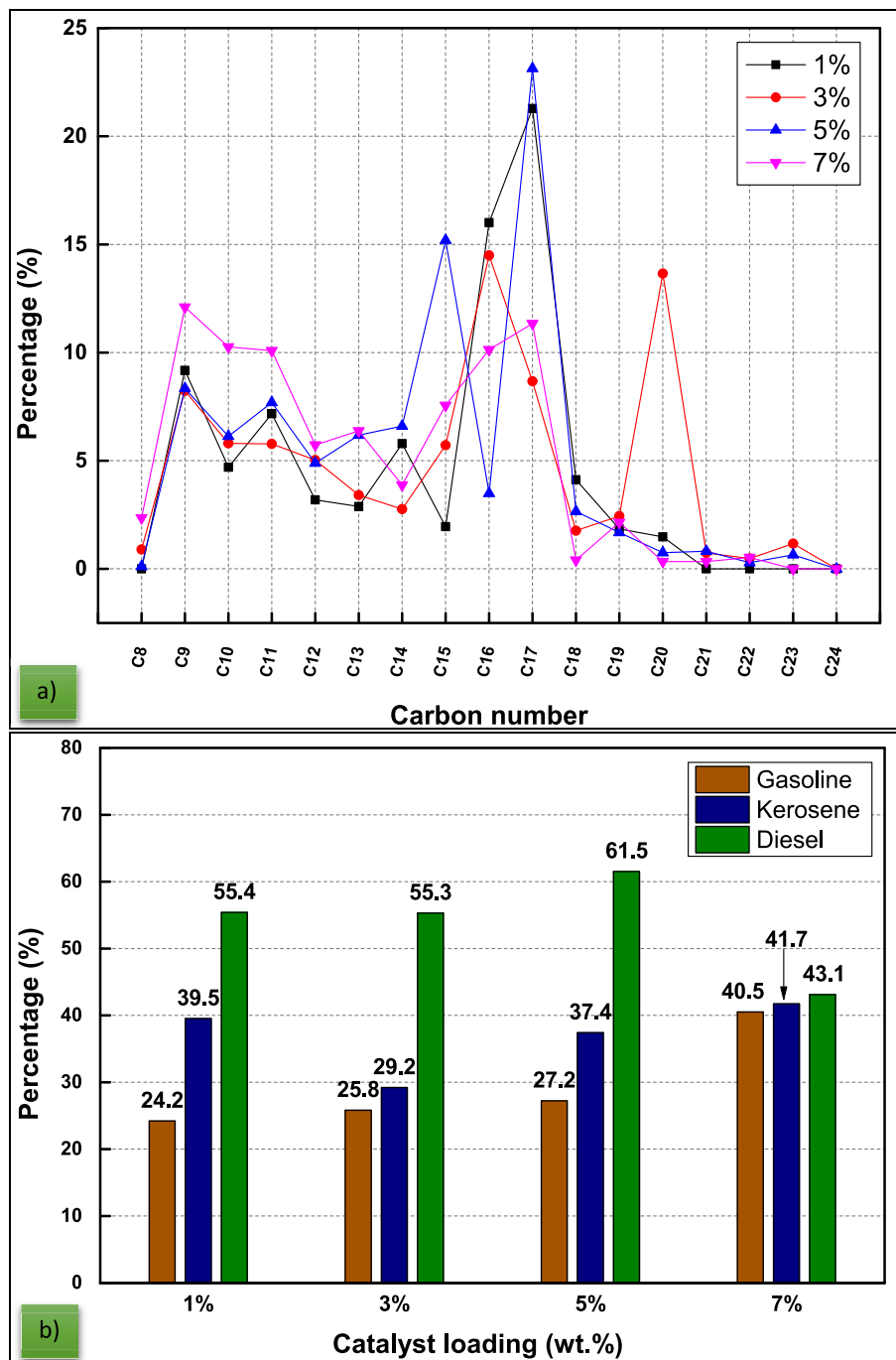

Fig. 13. (A) Product selectivity based on carbon number of hydrocarbon and b) selectivity towards gasoline, kerosene and diesel range fuel under different catalyst loading.

catalyst. Consequently, a catalyst loading of 5 wt% proved to be the most advantageous and economical for the deoxygenation process, resulting in a higher yield of green diesel and hydrocarbon compound.

The utilisation of NiO-CD as a catalyst in these deoxygenation reactions facilitates the generation of a diverse array of hydrocarbon biofuel, characterised by varying volatility and sizes. The biofuel fraction distribution exhibited a prevalence of higher yields within the diesel range. At 5 wt% of catalyst loading will favored to higher diesel range with 61.5 %. Fig. 13(b) shows that the increasing of NiO-CD catalyst loading will lead to increasing of hydrocarbon in the gasoline range (C_8-C_{12}) due cracking reaction of C-C bond was the favorable reaction in producing lighter hydrocarbon. The analysis of product distribution showed that increasing the catalyst loading from 1 to 7 wt% resulted in an expansion of the diverse array of hydrocarbons present in the biofuel. Based on the results, 5 wt% NiO-CD catalyst loading was determined to be suitable and cost-effective.

Conclusion

The low-cost NiO-CD catalyst demonstrates great potential as a catalyst for the deoxygenation of soybean oil (SO), resulting in the production of green diesel-like hydrocarbons. This catalyst outperforms commercial zeolite-based catalysts in terms of cost and efficiency. The NiO-CD catalyst exhibited the highest potential as a catalyst, resulting in the maximum yield of green diesel (50.5 wt%) and efficiency of oxygenated compound removal around 88.6 % which contributed higher yield of hydrocarbon compound (88.63 %). The successful dispersion of nickel metal onto calcined dolomite catalyst not only provides a more active site for catalysing SO reactant particles, but it also improves the thermal stability, particle size and textural mesoporosity of the synthesised NiO-CD catalyst. In addition, the existence of NiO species enhances the creation of acidic sites on the surface of the dolomite support catalyst system, leading to a synergistic effect of bifunctional acid-base characteristics of the synthesized low-cost NiO-CD catalyst. The majority of hydrocarbon products in catalytic deoxygenation (CDO) using NiO-CD catalyst are in the C_{15} and C_{17} hydrocarbon fractions because of dominant decarboxylation/decarbonylation (deCOx) reaction with high selectivity towards diesel range fuel. The study employed the one-factor-at-a-time (OFAT) approach to examine the impact of the NiO-CD catalyst in CDO of SO. A series of experiments found that catalyst loading had a significant impact on green diesel yield, hydrocarbon percentage, and the chemical composition. The optimal catalyst loading for the deoxygenation reaction of SO was determined to be 5 wt%. This resulted in the maximum yield of green diesel, which contributed to 50.5 wt% of the final product. Furthermore, the green diesel obtained had the highest hydrocarbon composition, with a percentage of 88.63 %. Thus, it was concluded that a catalyst loading of 5 wt% NiO-CD proves to be acceptable and cost-effective for the production of green diesel by the CDO of SO.

CRediT authorship contribution statement

R.S.R.M. Hafriz: Conceptualization, Investigation, Methodology, Software, Formal analysis, Validation, Data curation, Visualization, Writing – original draft. **S.H. Habib:** Writing – review & editing, Validation, Investigation, Conceptualization. **N.A. Raof:** Writing – review & editing, Validation, Investigation, Conceptualization. **M.Y. Ong:** Writing – review & editing. **C.C. Seah:** Validation, Data curation. **S.Z. Razali:** Resources, Project administration. **R. Yunus:** Validation, Supervision, Resources, Project administration. **N.M. Razali:** Resources, Project administration. **A. Salmiaton:** Writing – review & editing, Validation, Resources, Project administration, Methodology, Funding acquisition, Conceptualization.

Declaration of competing interest

The authors declare that they have no known competing financial interests or personal relationships that could have appeared to influence the work reported in this paper.

Data availability

Data will be made available on request.

Acknowledgements

References

[1] Labeckas G, Slavinskas S. Comparative evaluation of the combustion process and emissions of a diesel engine operating on the cetane improver 2-ethylhexyl nitrate doped rapeseed oil and aviation JP-8 Fuel. Energy Convers Manage: X 2021;11. https://doi.org/10.1016/j.ecmx.2021.100106.

[2] Afiqah-Idrus A, Abdulkareem-Alsultan G, Asikin-Mijan N, Fawzi Nassar M, Voon L, Hwa TS. Deoxygenation of waste sludge palm oil into hydrocarbon rich fuel over carbon-supported bimetallic tungsten-lanthanum catalyst. Energy Convers Manage X 2024;23. https://doi.org/10.1016/j.ecmx.2024.100589.

[3] Cremonez PA, Teleken JG, Weiser MT. Potential of green diesel to complement the brazilian energy production: a review. Energy Fuel 2021;35:176–86. https://doi.org/10.1021/acs.energyfuels.0c03805.

[4] Azman NS, Marliza TS, Asikin-Mijan N, Hin TYY, Khairuddin N. Production of biodiesel from waste cooking oil via deoxygenation using Ni-Mo/AC catalyst. Processes 2021;9. https://doi.org/10.3390/pr9050750.

[5] Di Vito NG, Gallucci K, Rossi L. Green diesel production by catalytic hydrodeoxygenation of vegetables oils. Int J Environ Res Public Health 2021;18. https://doi.org/10.3390/ijerph182413041.

[6] Bergmann JC, Tupinambá DD, Costa OYA, Almeida JRM, Barreto CC, Quirino BF. Biodiesel production in brazil and alternative biomass feedstocks. Renew Sustain Energy Rev 2013;21:411–20. https://doi.org/10.1016/j.rser.2012.12.058.

[7] Maciel VG, Zortea RB, Menezes Da Silva W, Cybis LFDA, Einloft S, Seferin M. Life cycle inventory for the agricultural stages of soybean production in the state of Rio Grande Do Sul, Brazil. J Clean Prod 2015;93(65–74). https://doi.org/10.1016/j.jclepro.2015.01.016.

[8] Timilsina GR, Chisari OO, Romero CA. Economy-wide impacts of biofuels in argentina. Energy Policy 2013;55:636–47. https://doi.org/10.1016/j.enpol.2012.12.060.

[9] Shehab M, Moshammer K, Franke M, Zondervan E. Analysis of the potential of meeting the eu's sustainable aviation fuel targets. Sustainability (switzerland) 2023;15. https://doi.org/10.3390/su15129266. in 2030 and 2050.

[10] Monteiro RRC, Dos Santos IA, Arcanjo MRA, Cavalcante CL, de Luna FMT, Fernandez-Lafuente R. Production of jet biofuels by catalytic hydroprocessing of esters and fatty acids. A Rev Catal 2022;12. https://doi.org/10.3390/catal12020237.

[11] Hebish AA, Zulkifli NWM, Julkapli NM, Patah MFA. The impact of operating conditions on h_2-free catalytic deoxygenation of triglycerides for bio-jet fuel synthesis: a step towards sustainable aviation. Appl Catal Open 2024;190:206926. https://doi.org/10.1016/j.apcato.2024.206926.

[12] Safa Gamal M, Asikin-Mijan N, Arumugam M, Rashid U, Taufiq-Yap YH. Solvent-free catalytic deoxygenation of palm fatty acid distillate over cobalt and manganese supported on activated carbon originating from waste coconut shell. J Anal Appl Pyrolysis 2019;144. https://doi.org/10.1016/j.jaap.2019.104690.

[13] Immer JG, Lamb HH. Fed-batch catalytic deoxygenation of free fatty acids. Energy Fuel 2010;24:5291–9. https://doi.org/10.1021/ef100576z.

[14] Lucantonio S, Di Giuliano A, Rossi L, Gallucci K. Green diesel production via deoxygenation process. A Review Energies (basel) 2023;16. https://doi.org/10.3390/en16020844.

[15] Pimenta JLCW, de Oliveira CM, Belo Duarte R, dos Santos OAA, de Matos Jorge LM. Deoxygenation of vegetable oils for the production of renewable diesel: improved aerogel based catalysts. Fuel 2021;290. https://doi.org/10.1016/j.fuel.2020.119979.

[16] Rahmawati Z, Santoso L, McCue A, Azua Jamari NL, Ninglasari SY, Gunawan T. Selectivity of reaction pathways for green diesel production towards biojet fuel applications. RSC Adv 2023;13:13698–714. https://doi.org/10.1039/d3ra02281a.

[17] Shi F, Wang H, Chen Y, Lu Y, Hou D, Liu C. Green diesel-like hydrocarbon production by h_2-free catalytic deoxygenation of oleic acid via Ni/MgO-Al$_2$O$_3$ catalysts: effect of the metal loading amount. J Environ Chem Eng 2023;11. https://doi.org/10.1016/j.jece.2023.110520.

[18] Choo MY, Oi LE, Ling TC, Ng EP, Lin YC, Centi G. Deoxygenation of triolein to green diesel in the H₂-free condition: effect of transition metal oxide supported on zeolite Y. J Anal Appl Pyrolysis 2020;147. https://doi.org/10.1016/j.jaap.2020.104797.

[19] Marinković DM, Pavlović SM. Recent advances in waste-based and natural zeolitic catalytic materials for biodiesel production. Hem Ind 2023;77:5–38. https://doi.org/10.2298/HEMIND220804007M.

[20] Ghorbannezhad P, Park S, Onwudili JA. Co-pyrolysis of biomass and plastic waste over zeolite- and sodium-based catalysts for enhanced yields of hydrocarbon products. Waste Manag 2020;102:909–18. https://doi.org/10.1016/j.wasman.2019.12.006.

[21] Hafriz RSRM, Shafizah IN, Arifin NA, Salmiaton A, Yunus R, Yap YHT. Effect of Ni/malaysian dolomite catalyst synthesis technique on deoxygenation reaction activity of waste cooking oil. Renew Energy 2021;178:128–43. https://doi.org/10.1016/j.renene.2021.06.074.

[22] Romero MJA, Pizzi A, Toscano G, Busca G, Bosio B, Arato E. Deoxygenation of waste cooking oil and non-edible oil for the production of liquid hydrocarbon biofuels. Waste Manage 2016;47:62–8. https://doi.org/10.1016/j.wasman.2015.03.033.

[23] Asikin-Mijan N, Lee HV, Juan JC, Noorsaadah AR, Abdulkareem-Alsultan G, Arumugam M. Waste clamshell-derived CaO supported Co and W catalysts for renewable fuels production via cracking-deoxygenation of triolein. J Anal Appl Pyrolysis 2016;120:110–20. https://doi.org/10.1016/j.jaap.2016.04.015.

[24] Santillan-Jimenez E, Morgan T, Shoup J, Harman-Ware AE, Crocker M. Catalytic deoxygenation of triglycerides and fatty acids to hydrocarbons over Ni-Al layered double hydroxide. Catal Today 2014;237:136–44. https://doi.org/10.1016/j.cattod.2013.11.009.

[25] Romero M, Pizzi A, Toscano G, Casazza AA, Busca G, Bosio B. Preliminary experimental study on biofuel production by deoxygenation of jatropha oil. Fuel Process Technol 2015;137:31–7. https://doi.org/10.1016/j.fuproc.2015.04.002.

[26] Hafriz RSRM, Salmiaton A, Yunus R, Taufiq-Yap YH. Green biofuel production via catalytic pyrolysis of waste cooking oil using malaysian dolomite catalyst. Bull Chem React Eng Catal 2018;13:489–501. https://doi.org/10.9767/bcrec.13.3.1956.489-501.

[27] Valle B, Aramburu B, Santiviago C, Bilbao J, Gayubo AG. Upgrading of bio-oil in a continuous process with dolomite catalyst. Energy Fuel 2014;28:6419–28. https://doi.org/10.1021/ef501600f.

[28] Buyang Y, Nugraha RE, Holilah H, Bahruji H, Suprapto S, Jalil AA. Dolomite catalyst for fast pyrolysis of waste cooking oil into hydrocarbon fuel. S Afr J Chem Eng 2023;45:60–72. https://doi.org/10.1016/j.sajce.2023.04.007.

[29] Lin Y, Zhang C, Zhang M, Zhang J. Deoxygenation of bio-oil during pyrolysis of biomass in the presence of cao in a fluidized-bed reactor. Energy Fuel 2010;24:5686–95. https://doi.org/10.1021/ef1009605.

[30] Kanchanatip E, Chansiriwat W, Palalerd S, Khunphonoi R, Kumsaen T, Wantala K. Light biofuel production from waste cooking oil via pyrolytic catalysis cracking over modified thai dolomite catalysts. Carbon Resour Convers 2022;5:177–84. https://doi.org/10.1016/j.crcon.2022.05.001.

[31] Tabandeh M, Cheng CK, Centi G, Show PL, Chen WH, Ling TC. Recent advancement in deoxygenation of fatty acids via homogeneous catalysis for biofuel production. Mol Catal 2022;523. https://doi.org/10.1016/j.mcat.2020.111207.

[32] Bjelić A, Grilc M, Huš M, Likozar B. Hydrogenation and hydrodeoxygenation of aromatic lignin monomers over Cu/C, Ni/C, Pd/C, Pt/C, Rh/C and Ru/C catalysts: mechanisms, reaction micro-kinetic modelling and quantitative structure-activity relationships. Chem Eng J 2019;359:305–20. https://doi.org/10.1016/j.cej.2018.11.107.

[33] Hongloi N, Prapainainar P, Prapainainar C. Review of green diesel production from fatty acid deoxygenation over ni-based catalysts. Mol Catal 2022;523. https://doi.org/10.1016/j.mcat.2021.111696.

[34] Khalit WNAW, Asikin-Mijan N, Marliza TS, Gamal MS, Shamsuddin MR, Saiman MI. Catalytic deoxygenation of waste cooking oil utilizing nickel oxide catalysts over various supports to produce renewable diesel fuel. Biomass Bioenergy 2021;154. https://doi.org/10.1016/j.biombioe.2021.106248.

[35] Adira Wan Khalit WN, Marliza TS, Asikin-Mijan N, Gamal MS, Saiman MI, Ibrahim ML. Development of Bimetallic Nickel-based Catalysts Supported on Activated Carbon for Green Fuel Production. RSC Adv. 2020, 10:37218–32. doi: 10.1039/d0ra06302a.

[36] Ambursa MM, Juan JC, Yahaya Y, Taufiq-Yap YH, Lin YC, Lee HV. A review on catalytic hydrodeoxygenation of lignin to transportation fuels by using nickel-based catalysts. Renew Sustain Energy Rev 2021;138. https://doi.org/10.1016/j.rser.2020.110667.

[37] Praserttaweeporn K, Vitidsant T, Charusiri W. Ni-modified dolomite for the catalytic deoxygenation of pyrolyzed softwood and non-wood to produce bio-oil. Results Eng 2022;14. https://doi.org/10.1016/j.rineng.2022.100461.

[38] Harith N, Hafriz RSRM, Arifin NA, Tan ES, Salmiaton A, Shamsuddin AH. Catalytic co-pyrolysis of blended biomass – plastic mixture using synthesized metal oxide(MO)-dolomite based catalyst. J Anal Appl Pyrolysis 2022;168. https://doi.org/10.1016/j.jaap.2022.105776.

[39] Hafriz RSRM, Nor Shafizah I, Salmiaton A, Arifin NA, Yunus R, Taufiq Yap YH. Comparative study of transition metal-doped calcined malaysian dolomite catalysts for WCO deoxygenation reaction. Arab J Chem 2020;13:8146–59. https://doi.org/10.1016/j.arabjc.2020.09.046.

[40] Hafriz RSRM, Habib SH, Raof NA, Razali SZ, Yunus R, Razali NM. The catalytic deoxygenation reaction temperature and N₂ gas flow rate influence the conversion of soybean fatty acids into green diesel. J Taiwan Inst Chem Eng 2024;165. https://doi.org/10.1016/j.jtice.2024.105700.

[41] Fan X. Furan formation from fatty acids as a result of storage, gamma irradiation UV-C and heat treatments. Food Chem 2015;175:439–44. https://doi.org/10.1016/j.foodchem.2014.12.002.

[42] Javed F, Shahbaz HM, Nawaz A, Olaimat AN, Stratakos AC, Wahyono A. Formation of Furan in Baby Food Products: Identification and Technical Challenges. Compr. Rev. Food Sci. Food (Saf). 2021, 20:2699–715. doi: 10.1111/1541-4337.12732.

[43] Kamil FH, Salmiaton A, Hafriz RSRM, Hussien IR, Omar R. Characterization and application of molten slag as catalyst in pyrolysis of waste cooking oil. Bull Chem React Eng Catal 2020;15:119–27. https://doi.org/10.9767/bcrec.15.1.3973.119-127.

[44] Hafriz RSRM, Arifin NA, Salmiaton A, Yunus R, Taufiq-Yap YH, Saifuddin NM. Multiple-objective Optimization in green fuel production via catalytic deoxygenation reaction with nio-dolomite catalyst. Fuel 2022;308. https://doi.org/10.1016/j.fuel.2021.122041.

[45] Alsultan GA, Asikin-Mijan N, Lee HV, Albazzaz AS, Taufiq-Yap YH. Deoxygenation of waste cooking to renewable diesel over walnut shell-derived nanorode activated carbon supported Cao-La₂O₃ catalyst. Energy Convers Manage 2017;151:311–23. https://doi.org/10.1016/j.enconman.2017.09.001.

[46] Asikin-Mijan N, Lee HV, Abdulkareem-Alsultan G, Afandi A, Taufiq-Yap YH. Production of green diesel via cleaner catalytic deoxygenation of jatropha curcas oil. J Clean Prod 2017;167:1048–59. https://doi.org/10.1016/j.jclepro.2016.10.023.

[47] Correia LM, de Sousa CN, Novaes DS, Cavalcante CL, Cecilia JA, Rodríguez-Castellón E. Characterization and application of dolomite as catalytic precursor for canola and sunflower oils for biodiesel production. Chem Eng J 2015;269:35–43. https://doi.org/10.1016/j.cej.2015.01.097.

[48] Muhammad WZW, Isa MR, Habib SH, Seah CC, Hafriz RSRM, Shamsuddin AH. Assessment of biochar, bio-oil and biogas production from lemon myrtle waste via microwave assisted catalytic pyrolysis using cao based catalyst and zeolite catalyst. Energy Convers Manage: x 2023;20. https://doi.org/10.1016/j.ecmx.2023.100481.

[49] Resio LC. Dolomite thermal behaviour: a proposal to establish a definitive decomposition mechanism in a convective air atmosphere. Open Ceramics 2023;15. https://doi.org/10.1016/j.oceram.2023.100405.

[50] Taufiq-Yap YH, Nur-Faizal AR, Sivasangar S, Hussein MZ, Aishah A. Modification of malaysian dolomite using mechanochemical treatment via different media for oil palm fronds gasification. Int J Energy Res 2014;38:1008–15. https://doi.org/10.1002/er.3118.

[51] Li C, Ma J, Xiao Z, Hector SB, Liu R, Zuo S. Catalytic Cracking of swida wilsoniana oil for hydrocarbon biofuel over Cu-modified ZSM-5 zeolite. Fuel 2018;218:59–66. https://doi.org/10.1016/j.fuel.2018.01.026.

[52] Emori EY, Hirashima FH, Zandonai CH, Ortiz-Bravo CA, Fernandes-Machado NRC, Olsen-Scaliante MHN. Catalytic cracking of soybean oil using ZSM5 zeolite. Catal Today 2017;279:168–76. https://doi.org/10.1016/j.cattod.2016.05.052.

[53] Ramli NAS, Amin NAS. Fe/HY zeolite as an effective catalyst for levulinic acid production from glucose: characterization and catalytic performance. Appl Catal b 2015;163:487–98. https://doi.org/10.1016/j.apcatb.2014.08.031.

[54] Ameen M, Azizan MT, Yusup S, Ramli A, Yasir M, Kaur H. H-Y zeolite as hydrodeoxygenation catalyst for diesel range hydrocarbon production from rubber seed oil. Mater Today: Proc 2019;16:1742–9.

[55] Xu J, Zhang T. Fabrication of spent FCC catalyst composites by loaded V₂O₅ and Tio₂ and their comparative photocatalytic activities. Sci Rep 2019;9. https://doi.org/10.1038/s41598-019-47155-y.

[56] Chen C, Yu J, Yoza BA, Li QX, Wang G. A novel "wastes-treat-wastes" technology: role and potential of spent fluid catalytic cracking catalyst assisted ozonation of petrochemical wastewater. J Environ Manage 2015;152:58–65. https://doi.org/10.1016/j.jenvman.2015.01.022.

[57] Yu F, Gao L, Wang W, Zhang G, Ji J. Bio-fuel production from the catalytic pyrolysis of soybean oil over Me-Al-MCM-41 (Me = La, Ni Or Fe) mesoporous materials. J Anal Appl Pyrolysis 2013;104:325–9. https://doi.org/10.1016/j.jaap.2013.06.017.

[58] Prihadiyono FI, Lestari WW, Putra R, Aqna ANL, Cahyani IS, Kadja GTM. Heterogeneous catalyst based on nickel modified into indonesian natural zeolite in green diesel production from crude palm oil. Int J Technol 2022;13:931–43. https://doi.org/10.14716/ijtech.v13i4.4695.

[59] Al-Jammal N, Al-Hamamre Z, Alnaief M. Manufacturing of zeolite based catalyst from zeolite tuft for biodiesel production from waste sunflower oil. Renew Energy 2016;93:449–59. https://doi.org/10.1016/j.renene.2016.03.018.

[60] Yuan P, Liu J, Li Y, Fan Y, Shi G, Liu H. Effect of pore diameter and structure of mesoporous sieve supported catalysts on hydrodesulfurization performance. Chem Eng Sci 2014;111:381–9. https://doi.org/10.1016/j.ces.2014.03.006.

[61] Ooi XY, Oi LE, Choo MY, Ong HC, Lee HV, Show PL. Efficient deoxygenation of triglycerides to hydrocarbon-biofuel over mesoporous Al₂O₃-Tio₂ catalyst. Fuel Process Technol 2019;194. https://doi.org/10.1016/j.fuproc.2019.106120.

[62] Wang YL, Zhang XC, Zhan GG, Wang MM, Li WQ, Pei CJ. Comparing the effects of hollow structure and mesoporous structure of ZSM-5 zeolites on catalytic performances in methanol aromatization. Mol Catal 2023;540. https://doi.org/10.1016/j.mcat.2023.113044.

[63] Qureshi KM, Kay Lup AN, Khan S, Abnisa F, Wan Daud WMA. Optimization of palm shell pyrolysis parameters in helical screw fluidized bed reactor: effect of particle size, pyrolysis time and vapor residence time. Clean Eng Technol 2021;4. https://doi.org/10.1016/j.clet.2021.100174.

[64] Basir NM, Jamil NAM, Hamdan H. Conversion of jet biofuel range hydrocarbons from palm oil over zeolite hybrid catalyst. Nanomater Nanotechnol 2021;11. https://doi.org/10.1177/1847980420981536.

[65] Dadashi M, Mazloom G, Akbari A, Banisharif F. The performance of micro-mesopore HY zeolite for supporting mo toward oxidation of dibenzothiophene. Environ Sci Pollut Res 2020;27:30600–14. https://doi.org/10.1007/s11356-020-09266-2.

[66] Ren J, Wang A, Li X, Chen Y, Liu H, Hu Y. Hydrodesulfurization of dibenzothiophene catalyzed by Ni-Mo sulfides supported on a mixture of MCM-41 and HY zeolite. Appl Catal A Gen 2008;344:175–82. https://doi.org/10.1016/j.apcata.2008.04.017.

[67] Ji Y, Yang H, Yan W. Strategies to enhance the catalytic performance of ZSM-5 zeolite in hydrocarbon cracking: a review. Catalysts 2017;7. https://doi.org/10.3390/catal7120367.

[68] Tani H, Hasegawa T, Shimouchi M, Asami K, Fujimoto K. Selective catalytic decarboxy-cracking of triglyceride to middle-distillate hydrocarbon. Catal Today 2011;164:410–4. https://doi.org/10.1016/j.cattod.2010.10.059.

[69] Chen L, Zhu Y, Zheng H, Zhang C, Li Y. Aqueous-phase hydrodeoxygenation of propanoic acid over the Ru/Zro₂ and Ru-Mo/Zro₂ Catalysts. Appl Catal A Gen 2012;411–412:95–104. https://doi.org/10.1016/j.apcata.2011.10.026.

[70] Daligaux V, Richard R, Manero MH. Deactivation and regeneration of zeolite catalysts used in pyrolysis of plastic wastes—A process and analytical review. Catalysts 2021;11. https://doi.org/10.3390/catal11070770.

[71] Wang F, Wang L, Zhu J, Zhang X, Yan Z, Fang F. Effect of Si/Al ratio of the starting nay on hydro-upgrading catalyst performance. Catal Today 2010;158: 409–14. https://doi.org/10.1016/j.cattod.2010.05.041.

[72] Saab R, Polychronopoulou K, Anjum DH, Charisiou ND, Goula MA, Hinder SJ. Effect of SiO₂/Al₂O₃ ratio in Ni/Zeolite-Y and Ni-W/Zeolite-Y catalysts on hydrocracking of heptane. Mol Catal 2022;528. https://doi.org/10.1016/j.mcat.2022.112484.

[73] Golubev IS, Dik PP, Kazakov MO, Pereyma VY, Klimov OV, Smirnova MY. The effect of Si/Al Ratio of zeolite Y in NiW catalyst for second stage hydrocracking. Catal Today 2021;378:65–74. https://doi.org/10.1016/j.cattod.2021.01.014.

[74] Leyva C, Trejo-Zárraga F. Effect of silicon content on active catalytic phase for hydrocracking of heavy crude oils. Pet Sci Technol 2020;38:91–7. https://doi.org/10.1080/10916466.2019.1671865.

[75] Jiang H. Silicon enrichment on iron contaminated fluid catalytic cracking catalyst particle surface. J Catal 2020;382:31–9. https://doi.org/10.1016/j.jcat.2019.12.013.

[76] Li J, Gao M, Yan W, Yu J. Regulation of the Si/Al ratios and Al distributions of zeolites and their impact on properties. Chem Sci 2022;14:1935–59. https://doi.org/10.1039/d2sc06010h.

[77] Li J, Liu M, Guo X, Dai C, Song C. Fluoride-mediated nano-sized high-silica ZSM-5 as an ultrastable catalyst for methanol conversion to propylene. J Energy Chem 2018;27:1225–30. https://doi.org/10.1016/j.jechem.2017.08.018.

[78] Shamsuddin MR, Asikin-Mijan N, Marliza TS, Miyamoto M, Uemiya S, Yarmo MA. Promoting dry reforming of methane via bifunctional NiO/dolomite catalysts for production of hydrogen-rich syngas. RSC Adv 2021;11:6667–81. https://doi.org/10.1039/d0ra09246k.

[79] Scaldaferri CA, Pasa VMD. Hydrogen-free process to convert lipids into bio-jet fuel and green diesel over niobium phosphate catalyst in one-step. Chem Eng J 2019;370:98–109. https://doi.org/10.1016/j.cej.2019.03.063.

[80] Valle B, Palos R, Bilbao J, Gayubo AG. Role of zeolite properties in bio-oil deoxygenation and hydrocarbons production by catalytic cracking. Fuel Process Technol 2022;227. https://doi.org/10.1016/j.fuproc.2021.107130.

[81] Gosselink RW, Hollak SAW, Chang SW, Van Haveren J, De Jong KP, Bitter JH. Reaction pathways for the deoxygenation of vegetable oils and related model compounds. ChemSusChem 2013;6:1576–94. https://doi.org/10.1002/cssc.201300370.

[82] Hermida L, Abdullah AZ, Mohamed AR. Deoxygenation of fatty acid to produce diesel-like hydrocarbons: a review of process conditions, reaction kinetics and mechanism. Renew Sustain Energy Rev 2015;42:1223–33. https://doi.org/10.1016/j.rser.2014.10.099.

[83] Dawes GJS, Scott EL, Le Nôtre J, Sanders JPM, Bitter JH. Deoxygenation of biobased molecules by decarboxylation and decarbonylation – a review on the role of heterogeneous. Homogeneous and Bio-Catalysis Green Chemistry 2015;17: 3231–50. https://doi.org/10.1039/c5gc00023h.

[84] Hafriz RSRM, Nor Shafizah I, Arifin NA, Maisarah AH, Salmiaton A, Shamsuddin AH. Comparative, reusability and regeneration study of potassium oxide-based catalyst in deoxygenation reaction of WCO. Energy Convers Manage: X 2022;13. https://doi.org/10.1016/j.ecmx.2021.100173.

[85] Sundus F, Fazal MA, Masjuki HH. Tribology with biodiesel: a study on enhancing biodiesel stability and its fuel properties. Renew Sustain Energy Rev 2017;70: 399–412. https://doi.org/10.1016/j.rser.2016.11.217.

[86] Zamri MFMA, Shamsuddin AH, Ali S, Bahru R, Milano J, Tiong SK. Recent advances of triglyceride catalytic pyrolysis via heterogenous dolomite catalyst for upgrading biofuel quality: a review. Nanomaterials 2023;13. https://doi.org/10.3390/nano13131947.

[87] Worldwide Fuel Charter Committee. Worldwide Fuel Charter, 6th Edition Gasoline and Diesel Fuel. 2019.

[88] Fahim MA, Alsahhaf TA, Elkilani A. Refinery feedstocks and products. fundamentals of petroleum refining. Elsevier 2010:11–31. https://doi.org/10.1016/b978-0-444-52785-1.00002-4.

[89] Idem RO, Katikaneni SPR, Bakhshi NN. Thermal cracking of canola oil: reaction products in the presence and absence of steam. Energy Fuels 1996;10(6): 1150–62.

[90] Aliana-Nasharuddin N, Asikin-Mijan N, Abdulkareem-Alsultan G, Saiman MI, Alharthi FA, Alghamdi AA. Production of green diesel from catalytic deoxygenation of chicken fat oil over a series binary metal oxide-supported MWCNTs. RSC Adv 2019;10:626–42. https://doi.org/10.1039/c9ra08409f.

[91] Pham TN, Sooknoi T, Crossley S, Resasco DE. Ketonization of carboxylic acids: mechanisms, catalysts, and applications in bio-oil upgrading. ACS Catal 2013;3 (11):2456–73.

[92] Altalhi A, Morsy SM, Abou Kana MTH, Negm NA, Mohamed EA. Pyrolytic Conversion of waste edible oil into biofuel using sulphonated modified alumina. Alex Eng J 2022;61:4847–61. https://doi.org/10.1016/j.aej.2021.10.038.

[93] Pimenta JLCW, Barreto RDT, dos Santos OAA, de Matos Jorge LM. Effects of reaction parameters on the deoxygenation of soybean oil for the sustainable production of hydrocarbons. Environ Prog Sustain Energy 2020;39. https://doi.org/10.1002/ep.13450.

[94] Baharudin KB, Taufiq-Yap YH, Hunns J, Isaacs M, Wilson K, Derawi D. Mesoporous NiO/Al-SBA-15 catalysts for solvent-free deoxygenation of palm fatty acid distillate. Microporous Mesoporous Mater 2019;276:13–22. https://doi.org/10.1016/j.micromeso.2018.09.014.

[95] Caceres-Martinez LE, Saavedra Lopez J, Dagle RA, Gillespie R, Kenttämaa HI, Kilaz G. Influence of blending cycloalkanes on the energy content, density, and viscosity of jet-A. Fuel 2024;358. https://doi.org/10.1016/j.fuel.2023.129986.

[96] Kwon KC, Mayfield H, Marolla T, Nichols B, Mashburn M. Catalytic deoxygenation of liquid biomass for hydrocarbon fuels. Renew Energy 2011;36: 907–15. https://doi.org/10.1016/j.renene.2010.09.004.

[97] Obeas LK, Ghalib A khalid, Abdulkareem-Alsultan G, Asikin-Mijan N, Yunus R, Taufiq-Yap YH. Highly Thermal Stable Catalyst for Deoxygenation Jatropha Oil under Free Hydrogen and Solvent for Hydrocarbons Like Diesel Fuel with Highly Thermal Flow Properties. European Chemical Bulletin. 2022, 11:93–103. doi: 10.31838/ecb/2022.11.04.014.

[98] Malvarinda F, Syakdani A, Taufik M. Production of green diesel based on palm fatty acid distillate using catalytic hydrogenation method. OISAA J Indonesia Emas 2022;5(2):128.

[99] Shi H, Chen J, Yang Y, Tian S. Catalytic deoxygenation of methyl laurate as a model compound to hydrocarbons on nickel phosphide catalysts: remarkable support effect. Fuel Process Technol 2014;118:161–70. https://doi.org/10.1016/j.fuproc.2013.08.010.

[100] Na JG, Yi BE, Kim JN, Yi KB, Park SY, Park JH. Hydrocarbon production from decarboxylation of fatty acid without hydrogen. Catal Today 2010;156:44–8. https://doi.org/10.1016/j.cattod.2009.11.008.

[101] Žula M, Grilc M, Hydrocracking LB. Hydrogenation and Hydro-deoxygenation of fatty acids, esters and glycerides: mechanisms, kinetics and transport phenomena. Chem Eng J 2022;444. https://doi.org/10.1016/j.cej.2022.136564.

[102] Abdel-Shafy HI, Mansour MSM. A review on polycyclic aromatic hydrocarbons: source, environmental impact, effect on human health and remediation. Egpt J Pet 2016;25:107–23. https://doi.org/10.1016/j.ejpe.2015.03.011.

[103] Shitao Y, Cao X, Wu S, Chen Q, Li L, Li H. Effective pyrolysis of waste cooking oils into hydrocarbon rich biofuel on novel mesoporous catalyst with acid and alkali coexisting. Ind Crops Prod 2020;150. https://doi.org/10.1016/j.indcrop.2020.112362.

[104] Wan Khalit WNA, Asikin-Mijan N, Marliza TS, Safa-Gamal M, Shamsuddin MR, Azreena IN. One-pot decarboxylation and decarbonylation reaction of waste cooking oil over activated carbon supported nickel-zinc catalyst into diesel-like fuels. J Anal Appl Pyrolysis 2022;164. https://doi.org/10.1016/j.jaap.2022.105505.